IMA Journal of Numerical Analysis (2012) **32** 926–956
doi:10.1093/imanum/drr001
Advance Access publication on July 17, 2011

Analysis of spatial high-order finite difference methods for Maxwell's equations in dispersive media

V. A. BOKIL* AND N. L. GIBSON
Department of Mathematics, Oregon State University, Corvallis, OR 97331-4605, USA
*Corresponding author: bokilv@math.oregonstate.edu gibsonn@math.oregonstate.edu

[Received on 19 January 2010; revised on 4 November 2010]

We study the stability properties of, and the phase error present in, several higher-order (in space) staggered finite difference schemes for Maxwell's equations coupled with a Debye or Lorentz polarization model. We present a novel expansion of the *symbol* of finite difference approximations, of arbitrary (even) order, of the first-order spatial derivative operator. This alternative representation allows the derivation of a concise formula for the numerical dispersion relation for all (even-) order schemes applied to each model, including the limiting (infinite-order) case. We further derive a closed-form analytical stability condition for these schemes as a function of the order of the method. Using representative numerical values for the physical parameters, we validate the stability criterion while quantifying numerical dissipation. Lastly, we demonstrate the effect that the spatial discretization order, and the corresponding stability constraint, has on the dispersion error.

Keywords: Maxwell's equations; Debye; Lorentz; higher-order FDTD; stability; dispersion.

1. Introduction

The computational simulation of electromagnetic interrogation problems, for the determination of the dielectric properties of complex dispersive materials (such as biological tissue), requires the use of highly efficient forward simulations of the propagation of transient electromagnetic waves in these media. These simulations have very important applications in diverse areas including noninvasive detection of cancerous tumours and the investigation of the effect of precursors on the human body (see Banks *et al*., 2000; Fear *et al*., 2003 and references therein). Thus, a lot of research has concentrated on the development of accurate, consistent and stable discrete forward solvers.

The electric and magnetic fields inside a material are governed by the macroscopic Maxwell's equations along with constitutive laws that account for the response of the material to the electromagnetic field. The complex electric permittivity of a dielectric medium is frequency dependent (has dielectric dispersion). Thus, an appropriate discretization method should have a numerical dispersion that matches the model dispersion as closely as possible. Dielectric materials also have physical dissipation or attenuation, which must also be correctly computed by a numerical method.

The Lax–Richtmyer theorem (see, e.g., Strikwerda, 2004) states that the convergence of consistent difference schemes to well-posed initial value problems represented by partial differential equations (PDEs) is equivalent to stability. Hence, analysis of stability criteria for conditionally stable schemes is important. The stability and dispersion properties for the finite-difference time-domain (FDTD) methods, also called Yee schemes, applied to Maxwell's equations in free space are well known (see Taflove & Hagness, 2005). There are several FDTD extensions that have been developed to model

electromagnetic pulse propagation in dispersive media. One way to model a dispersive medium is to add to Maxwell's equations a set of ordinary differential equations (ODEs) that relate the electric displacement **D** to the electric field **E** as done in Joseph *et al.* (1991) or a set of ODEs that model the dynamic evolution of the macroscopic polarization vector **P** driven by the electric field as done in Kashiwa *et al.* (1990) and Kashiwa & Fukai (1990). This technique is known as the auxiliary differential equation (ADE) method. Yee schemes are constructed for this augmented system by discretizing Maxwell's equations as usual and, in addition, time discretizing the auxiliary ODEs using a second-order method in time, so that the fully discretized augmented Maxwell system is second-order accurate in space and time. There are other modelling approaches that are also available (see Siushansian & LoVetri, 1995; Taflove & Hagness, 2005 and references therein). The discrete versions of many of these modelling approaches have been analysed for their numerical errors and stability properties in Petropoulos (1994); Siushansian & LoVetri (1995); Young *et al.* (1995); Cummer (1997); Young & Nelson (2001) and Bidégaray-Fesquet (2008).

In this paper we consider Maxwell's equations in Debye or Lorentz dispersive media using the ADE approach and analyse high-order (in space) staggered Yee-like methods for the numerical discretization of the augmented Maxwell system. These methods have $2M$-order accuracy in space for $M \in \mathbb{N}$ and second-order accuracy in time. We denote such methods as $(2, 2M)$-order finite difference methods.

Higher order staggered finite difference methods for approximating Maxwell's equations in dispersive media have been considered in Young (1996); Young *et al.* (1997); Prokopidis *et al.* (2004) and Prokopidis & Tsiboukis (2004, 2006). In particular, in Young (1996) and Young *et al.* (1997), a (4,4) method for Maxwell's equations in a cold plasma was developed, while in Prokopidis & Tsiboukis (2004), Prokopidis *et al.* (2004) and Prokopidis & Tsiboukis (2006), various (2,2)-, (2,4)- and (2,6)-order methods for Debye, Drude and Lorentz media were considered. In Petropoulos (1995) the author presents arguments in favour of using (2,4)-order finite difference schemes for wave propagation in Debye media. Caution should be used with higher-order finite difference methods, however, especially when applied to discontinuous material parameters or when using nonperiodic boundary conditions (see Fornberg, 1990).

Our focus in this paper is the derivation of closed-form analytical stability criteria for staggered $(2, 2M)$ finite difference methods, for arbitrary $M \in \mathbb{N}$, including the limiting infinite-order method. In addition, we also derive numerical dispersion relations for these schemes. The outline of the paper is as follows. In Section 2 we describe the ADE formulations for Debye and Lorentz type dispersive media in three dimensions, and in Section 3 we consider the one-dimensional models. The key result required to perform the stability and dispersion analyses for arbitrary M is the equivalence of the symbol of the $2M$-order finite difference approximation of the first-order derivative operator $\partial/\partial z$ with the truncation of an appropriate series expansion of the symbol of $\partial/\partial z$. This result is proved in Section 4. A similar result has been proved for $2M$-order finite difference approximations of the Laplace operator in Anne *et al.* (2000), which also enabled the authors to derive closed-form stability conditions and dispersion relations for $(2, 2M)$ schemes applied to the one-dimensional wave equation.

The $(2, 2M)$-order schemes for Debye and Lorentz media are presented in Section 5. In conjunction with the key result obtained in Section 4, von Neumann analysis is used to obtain stability conditions in Section 6. In Petropoulos (1994) the author derived partial stability conditions and numerical dispersion relations for the $(2, 2)$ schemes for Debye and Lorentz dispersive media. These results were confirmed for certain representative media for each model. In Bidégaray-Fesquet (2008) the stability analysis was extended and stability conditions for the $(2, 2)$ schemes for general Debye and Lorentz dispersive media were derived using von Neumann analysis. We use the ideas and results from Bidégaray-Fesquet (2008)

and Petropoulos (1994) and extend the stability analysis to $(2, 2M)$-order staggered finite difference methods. In Section 7 we extend the numerical dispersion analysis in Petropoulos (1994) to $(2, 2M)$ schemes. Numerical dispersion relations were not considered in Bidégaray-Fesquet (2008). Stability conditions for the $(2, 4)$ methods for Debye and Lorentz media were derived in Prokopidis & Tsiboukis (2004) using the Routh–Hurwitz criteria and numerical dispersion relations were also considered for the cases $2M = 2, 4, 6$. The numerical dispersion analysis was extended to arbitrary (even-) order methods in Prokopidis & Tsiboukis (2006), however, the representations used led to cumbersome algebra, and the extension to the limiting (infinite-order) case is not obvious.

The stability and dispersion analyses performed in this paper are for one-dimensional models. However, from these results, the extension to two and three dimensions, though tedious, can be easily performed. We present conclusions in Section 8.

2. Model formulation

We consider the Maxwell curl equations, which govern the electric field $\mathbf{E}$ and the magnetic field $\mathbf{H}$ in a domain Ω with no free charges in the time interval $(0, T)$, given as

$$\frac{\partial \mathbf{D}}{\partial t} - \frac{1}{\mu_0} \nabla \times \mathbf{B} = \mathbf{0} \quad \text{in } (0, T) \times \Omega, \tag{2.1a}$$

$$\frac{\partial \mathbf{B}}{\partial t} + \nabla \times \mathbf{E} = \mathbf{0} \quad \text{in } (0, T) \times \Omega. \tag{2.1b}$$

The fields $\mathbf{D}$ and $\mathbf{B}$ are the electric and magnetic flux densities, respectively. All the fields in (2.1) are functions of position $\mathbf{x} = (x, y, z)$ and time t. We neglect the effects of boundary conditions and initial conditions.

We will consider the case of a dispersive dielectric medium in which magnetic effects are negligible. Thus, within the dielectric medium, we have constitutive relations that relate the flux densities $\mathbf{D}$ and $\mathbf{B}$ to the electric and magnetic fields, respectively, as

$$\mathbf{D} = \epsilon_0 \epsilon_\mathrm{r} \mathbf{E} + \mathbf{P}, \tag{2.2a}$$

$$\mathbf{B} = \mu_0 \mathbf{H}. \tag{2.2b}$$

The parameters ϵ_0 and μ_0 are the permittivity and permeability, respectively, of free space. The field vector $\mathbf{P}$ is called the macroscopic electric polarization, and the parameter ϵ_r is the relative permittivity of the dielectric. The constitutive relations (2.2) describe the response of a material to the electromagnetic fields.

In this paper we concentrate our analyses on single-pole Debye and Lorentz polarization models, although the methods can be easily extended to multi-pole models.

2.1 *Orientational polarization: the Debye model*

A (single-pole) Debye model can be represented in (macroscopic) differential form (see, e.g., Kashiwa *et al*., 1990; Joseph *et al*., 1991) as

$$\epsilon_0 \epsilon_\infty \tau \frac{\partial \mathbf{E}}{\partial t} + \epsilon_0 \epsilon_\mathrm{s} \mathbf{E} = \tau \frac{\partial \mathbf{D}}{\partial t} + \mathbf{D}. \tag{2.3}$$

In equation (2.3), the parameter ϵ_s is the static relative permittivity. The presence of instantaneous polarization is accounted for by the coefficient $\epsilon_r = \epsilon_\infty$, the infinite frequency permittivity, in the electric flux equation (2.2a) and in the Debye model (2.3). The difference between these permittivities is commonly written $\epsilon_d := \epsilon_s - \epsilon_\infty$. The electric polarization, less the part included in the instantaneous polarization, can be understood to be a decaying exponential with relaxation parameter τ, which is driven by the electric field.

An alternate formulation of a Debye model exists where an ODE, describing the dynamic evolution of the macroscopic polarization $\mathbf{P}$ driven by the electric field, is augmented to the Maxwell system. As shown in Petropoulos (1994) and Bidégaray-Fesquet (2008), the discrete (2, 2)-order finite difference method for this alternate formulation has identical stability and dispersion properties to the discrete (2, 2)-order finite difference method based on equation (2.3). Thus, we do not consider this alternate formulation here.

2.2 *Electronic polarization: the Lorentz model*

A (single-pole) Lorentz model can be represented in (macroscopic) differential form (see, e.g., Banks *et al.*, 2000) as

$$\frac{\partial^2 \mathbf{P}}{\partial t^2} + \nu \frac{\partial \mathbf{P}}{\partial t} + \omega_0^2 \mathbf{P} = \epsilon_0 \omega_p^2 \mathbf{E}, \tag{2.4}$$

along with equation (2.2a). In (2.4), the plasma frequency ω_p is defined as $\omega_p := \omega_0 \sqrt{\epsilon_d}$, where $\epsilon_d := \epsilon_s - \epsilon_\infty$ with ϵ_s and ϵ_∞ as defined for the Debye model. The parameter ω_0 is the resonance frequency of the material, while ν is a damping coefficient.

Combining the equations (2.4) and (2.2a) results in an alternate formulation (see Joseph *et al.*, 1991) for a Lorentz material given as

$$\epsilon_0 \epsilon_\infty \frac{\partial^2 \mathbf{E}}{\partial t^2} + \epsilon_0 \epsilon_\infty \nu \frac{\partial \mathbf{E}}{\partial t} + \epsilon_0 \epsilon_s \omega_0^2 \mathbf{E} = \frac{\partial^2 \mathbf{D}}{\partial t^2} + \nu \frac{\partial \mathbf{D}}{\partial t} + \omega_0^2 \mathbf{D}. \tag{2.5}$$

Another alternative representation for a Lorentz material is to couple (2.2a) with (2.4) rewritten as a system of first-order equations (see Kashiwa & Fukai, 1990) by defining $\frac{\partial \mathbf{P}}{\partial t} = \mathbf{J}$ to get

$$\frac{\partial \mathbf{P}}{\partial t} = \mathbf{J}, \tag{2.6a}$$

$$\frac{\partial \mathbf{J}}{\partial t} + \nu \mathbf{J} + \omega_0^2 \mathbf{P} = \epsilon_0 \omega_p^2 \mathbf{E}. \tag{2.6b}$$

3. Reduction to one dimension

We consider the one-dimensional case in which the electric field is assumed to be polarized to oscillate in the y direction and propagates in the z direction. For any field vector $\mathbf{V}(t, \mathbf{x})$, we can write

$$\mathbf{V}(t, \mathbf{x}) = \hat{e}_d V(t, z), \tag{3.1}$$

where $\hat{e}_d$ is a unit vector in the d direction, and $V(t, z)$ is a scalar function of t and z. If $\mathbf{V} = \mathbf{E}, \mathbf{D}, \mathbf{P}$ or $\mathbf{J}$, then $d = y$ as all these field quantities oscillate in the y direction. If $\mathbf{V} = \mathbf{H}$ or $\mathbf{B}$, then $d = x$ as the magnetic field and flux density oscillate in the x direction. All the fields propagate in the z direction. Thus, we are only concerned with the scalar values $E(t, z)$, $H(t, z)$, $D(t, z)$, $B(t, z)$, $P(t, z)$ and $J(t, z)$.

In this case Maxwell's equations (2.1) in the interior of the domain Ω become

$$\frac{\partial B}{\partial t} = \frac{\partial E}{\partial z}, \tag{3.2a}$$

$$\frac{\partial D}{\partial t} = \frac{1}{\mu_0}\frac{\partial B}{\partial z}. \tag{3.2b}$$

Using the constitutive law (2.2a) in one dimension, we can rewrite Ampère's law, (3.2b), as

$$\epsilon_0\epsilon_\infty \frac{\partial E}{\partial t} + \frac{\partial P}{\partial t} = \frac{1}{\mu_0}\frac{\partial B}{\partial z}. \tag{3.3}$$

4. 2*M*-order spatial approximations

In this section we describe the construction of higher-order approximations to the first-order derivative operator $\partial/\partial z$. The construction presented in this section uses the notation from Cohen (2001) and Anne *et al*. (2000).

4.1 *Staggered ℓ^2 normed spaces*

Following the notation in Cohen (2001, p. 36) we introduce the following staggered ℓ^2 normed spaces that will aid in obtaining the basic properties of the high-order approximations. We define the *primary grid*, G_{p}, of $\mathbb{R}$ and the *dual grid*, G_{d}, of $\mathbb{R}$ both with space step size h to be

$$G_{\mathrm{p}} = \{\ell h | \ell \in \mathbb{Z}\} \quad \text{and} \quad G_{\mathrm{d}} = \left\{\left(\ell + \frac{1}{2}\right)h | \ell \in \mathbb{Z}\right\}, \tag{4.1}$$

respectively. For any function v, we denote $v_\ell = v(\ell h)$ and $v_{\ell+\frac{1}{2}} = v\big(\big(\ell+\frac{1}{2}\big)h\big)$. We define staggered ℓ^2 normed spaces on G_{p} and G_{d}, respectively, as $V_0 = \left\{(v_\ell), \ell \in \mathbb{Z} | h\sum_{\ell\in\mathbb{Z}} |v_\ell|^2 \leqslant \infty\right\}$, and $V_{\frac{1}{2}} = \left\{\big(v_{\ell+\frac{1}{2}}\big), \ell \in \mathbb{Z} | h\sum_{\ell\in\mathbb{Z}} |v_{\ell+\frac{1}{2}}|^2 \leqslant \infty\right\}$, with scalar products $(\cdot,\cdot)_0$ and $(\cdot,\cdot)_{\frac{1}{2}}$ derived from the norms $\|v\|_0^2 = h\sum |v_\ell|^2$ and $\|v\|_{\frac{1}{2}}^2 = h\sum \big|v_{\ell+\frac{1}{2}}\big|^2$.

Next, we define the discrete operators

$$\mathscr{D}_{p,h}^{(2)}\colon V_0 \to V_{\frac{1}{2}} \text{ defined by } \left(\mathscr{D}_{p,h}^{(2)}u\right)_{\ell+\frac{1}{2}} = \frac{u_{\ell+p} - u_{\ell-p+1}}{(2p-1)h},$$

$$\tilde{\mathscr{D}}_{p,h}^{(2)}\colon V_{\frac{1}{2}} \to V_0 \text{ defined by } \left(\tilde{\mathscr{D}}_{p,h}^{(2)}u\right)_{\ell} = \frac{u_{\ell+p-\frac{1}{2}} - u_{\ell-p+\frac{1}{2}}}{(2p-1)h}.$$

These are second-order discrete approximations of the operator $\partial/\partial z$ computed with step size $(2p-1)h$.

REMARK 4.1 If we denote $\mathscr{D}^*$ to be the adjoint of the discrete operator $\mathscr{D}$ for the ℓ^2 scalar product, we can note that $\tilde{\mathscr{D}}_{p,h}^{(2)} = -\left(\mathscr{D}_{p,h}^{(2)}\right)^*$, (cf., Cohen, 2001, p. 37).

If $u \in C^{2m+3}(\mathbb{R})$, with m an integer, and $m \geqslant 1$, we have the following Taylor expansions (cf., Cohen, 2001, p. 53)

$$\left(\tilde{\mathscr{D}}^{(2)}_{1,h}u\right)_\ell = \frac{\partial u_\ell}{\partial z} + \sum_{i=1}^{m} \frac{h^{2i}}{(2i+1)!2^{2i}} \frac{\partial^{2i+1}u_\ell}{\partial z^{2i+1}} + \mathcal{O}\left(h^{2m+2}\right), \tag{4.2}$$

$$\left(\mathscr{D}^{(2)}_{1,h}u\right)_{\ell+\frac{1}{2}} = \frac{\partial u_{\ell+\frac{1}{2}}}{\partial z} + \sum_{i=1}^{m} \frac{h^{2i}}{(2i+1)!2^{2i}} \frac{\partial^{2i+1}u_{\ell+\frac{1}{2}}}{\partial z^{2i+1}} + \mathcal{O}\left(h^{2m+2}\right). \tag{4.3}$$

4.2 *Two different ways of constructing finite difference approximations*

Following the work done in Anne *et al*. (2000) we construct finite difference approximations of order $2M$ of the first-order operator $\partial/\partial z$, where $M \in \mathbb{N}$ is arbitrary. These approximations will be denoted

$$\mathscr{D}^{(2M)}_{1,h}\colon V_0 \to V_{\frac{1}{2}}, \quad \tilde{\mathscr{D}}^{(2M)}_{1,h}\colon V_{\frac{1}{2}} \to V_0. \tag{4.4}$$

The operators in (4.4) can be considered from two different points of view (see Anne *et al*., 2000):

(V1) as linear combinations of second-order approximations to $\partial/\partial z$ computed with different space steps and

(V2) as a result of the truncation of an appropriate series expansion of the symbol of the operator $\partial/\partial z$.

In Anne *et al*. (2000) these two viewpoints were adopted for construction of finite difference approximations to the Laplace operator.

4.2.1 *Linear combinations of second-order approximations to* $\partial/\partial z$.

In the case of (V1) if we consider the linear combinations

$$\mathscr{D}^{(2M)}_{1,h} = \sum_{p=1}^{M} \lambda^{2M}_{2p-1}\mathscr{D}^{(2)}_{p,h}, \quad \tilde{\mathscr{D}}^{(2M)}_{1,h} = \sum_{p=1}^{M} \lambda^{2M}_{2p-1}\tilde{\mathscr{D}}^{(2)}_{p,h}, \tag{4.5}$$

then one can show that (see Cohen, 2001, p. 53 and Bokil & Gibson, 2010) the coefficients λ^{2M}_{2p-1} are given by the following explicit formula.

THEOREM 4.2 For any $M \in \mathbb{N}$, the coefficients λ^{2M}_{2p-1} of the linear combinations (4.5) are given by the explicit formula

$$\lambda^{2M}_{2p-1} = \frac{2(-1)^{p-1}[(2M-1)!!]^2}{(2M+2p-2)!!(2M-2p)!!(2p-1)}, \tag{4.6}$$

where $1 \leqslant p \leqslant M$, and the double factorial is defined as

$$n!! = \begin{cases} n\cdot(n-2)\cdot(n-4),\ldots,5\cdot3\cdot1, & n>0,\ \text{odd},\\ n\cdot(n-2)\cdot(n-4),\ldots,6\cdot4\cdot2, & n>0,\ \text{even},\\ 1, & n=-1,0. \end{cases} \tag{4.7}$$

REMARK 4.3 Theorem 4.2 may be proven using a technique analogous to that used in the proof of Theorem 1.1 in Anne *et al*. (2000) (see Bokil & Gibson, 2010). The result in (4.6) has been obtained, using other techniques, by other authors in the past (see Fornberg, 1975; Fornberg & Ghrist, 1999; Ghrist, 2000). In Anne *et al*. (2000) the authors prove several additional properties of the corresponding coefficients for higher-order approximations of the Laplace operator. Similar properties for the coefficients λ_{2p-1}^{2M} can be proved. Some of these properties have been proved in Ghrist (2000) and Fornberg & Ghrist (1999).

4.2.2 *Series expansion of the symbol of the operator $\partial/\partial z$.* With respect to the second point of view, (V2), we can interpret the operators $\mathscr{D}_{1,h}^{(2M)}$ and $\tilde{\mathscr{D}}_{1,h}^{(2M)}$ via their *symbols* (cf., Anne *et al*., 2000). We define the symbol of a differential operator, as well as its finite difference approximation, via its application to harmonic plane waves. Thus, if $v(z) = \mathrm{e}^{\mathrm{i}kz}$, then $\partial v/\partial z = \mathrm{i}kv(z)$, and

$$\mathscr{F}(\partial/\partial z) = \mathrm{i}k, \tag{4.8}$$

where $\mathscr{F}(\partial/\partial z)$ denotes the symbol of the differential operator $\partial/\partial z$. Similarly, we can show that the symbol of the finite difference operator $\tilde{\mathscr{D}}_{1,h}^{(2M)}$ can be written as

$$\mathscr{F}\left(\tilde{\mathscr{D}}_{1,h}^{(2M)}\right) = \frac{2\mathrm{i}}{h}\sum_{j=1}^{M}\frac{\lambda_{2j-1}^{2M}}{2j-1}\sin(kh(2j-1)/2). \tag{4.9}$$

We now introduce the following alternative formulation for the symbol of the operator $\tilde{\mathscr{D}}_{1,h}^{(2M)}$.

THEOREM 4.4 The symbol of the operator $\tilde{\mathscr{D}}_{1,h}^{(2M)}$ can be rewritten in the form

$$\mathscr{F}\left(\tilde{\mathscr{D}}_{1,h}^{(2M)}\right) = \frac{2\mathrm{i}}{h}\sum_{p=1}^{M}\gamma_{2p-1}\sin^{2p-1}(kh/2), \tag{4.10}$$

where the coefficients γ_{2p-1} are strictly positive, independent of M, and are given by the explicit formula

$$\gamma_{2p-1} = \frac{[(2p-3)!!]^2}{(2p-1)!}. \tag{4.11}$$

Proof. We follow an analogous proof in Anne *et al*. (2000) for approximations of the Laplace operator. Let us define $K := kh/2$. Since $\tilde{\mathscr{D}}_{1,h}^{(2M)}$ is of order $2M$, the difference in the symbols of $\partial/\partial z$ and the symbol of $\tilde{\mathscr{D}}_{1,h}^{(2M)}$ must be of $\mathcal{O}(K^{2M})$ for small K. Thus,

$$\mathscr{F}\left(\frac{\partial}{\partial z}\right) = \mathrm{i}k = \frac{2\mathrm{i}K}{h} = \frac{2\mathrm{i}}{h}\left(\sum_{p=1}^{M}\gamma_{2p-1}\sin^{2p-1}K + \mathcal{O}\left(K^{2M+1}\right)\right). \tag{4.12}$$

This implies that the γ_{2p-1} are the first M coefficients of a series expansion of K in terms of $\sin K$. Set $x = \sin K$ for $|K| < \pi/2$. Then, $K = \sin^{-1}x$ where $x \in (-1, 1)$ with

$$K = \sin^{-1}x = \sum_{p=1}^{M}\gamma_{2p-1}x^{2p-1} + \mathcal{O}\left(x^{2M+1}\right). \tag{4.13}$$

Requiring that equation (4.13) be true $\forall\, M \in \mathbb{N}$ implies that if a solution exists for $\{\gamma_{2p-1}\}_{p=1}^{M}$, then it is unique. We note that the function $Y(x) = \sin^{-1} x$ obeys the differential equation

$$(1 - x^2)Y'' - xY' = 0 \quad \text{where} \quad x \in (-1, 1), \tag{4.14}$$

with the conditions

$$Y(0) = 0, \quad Y'(0) = 1. \tag{4.15}$$

Substituting, formally, the series expansion $Y(x) = \sum_{p=1}^{\infty} \gamma_{2p-1} x^{2p-1}$ into (4.14), we obtain the equation $(6\gamma_3 - \gamma_1) + \sum_{p=2}^{\infty} \beta_{2p-1} x^{2p-1} = 0$, where $\beta_{2p-1} = (2p+1)(2p)\gamma_{2p+1} - (2p-1)^2\gamma_{2p-1}$. This implies that $\gamma_3 = \frac{1}{6}\gamma_1$, and

$$\gamma_{2p+1} = \frac{(2p-1)^2}{(2p)(2p+1)}\gamma_{2p-1}, \tag{4.16}$$

which gives us the formula $\gamma_{2p-1} = \frac{[(2p-3)!!]^2}{(2p-1)!}\gamma_1$. From the conditions (4.15) we see that $\gamma_1 = 1$, so that we finally obtain the formula (4.11). □

REMARK 4.5 We note that the relation (4.16) gives

$$\lim_{p\to\infty} \frac{\gamma_{2p+1}}{\gamma_{2p-1}} = 1. \tag{4.17}$$

This justifies the term-by-term differentiation of the series expansion of Y on $(-1, 1)$ in the proof of Theorem 4.4.

REMARK 4.6 To our knowledge, the result obtained in Theorem 4.4 is new and has not been proven elsewhere. It is this result that is key to obtaining closed-form analytical stability and dispersion formulae for the $(2, 2M)$ finite difference methods in Sections 6 and 7, respectively.

REMARK 4.7 We note that the coefficients γ_{2p-1}, defined in (4.11), are the coefficients in the Taylor expansion of the function $\sin^{-1} x$ around zero.

LEMMA 4.8 The series $\sum_{p=1}^{\infty} \gamma_{2p-1}$ is convergent and its sum is $\pi/2$.

Proof. The proof is straightforward. See Bokil & Gibson (2010) for details. □

In Table 1 we provide the coefficients γ_{2p-1} for representing the $2M$-order finite difference approximation to the operator $\partial/\partial z$ for various values of p. A similar table of values for the coefficients λ_{2p-1}^{2M} for various M and p can be found in Cohen (2001, p. 54).

Finally, we show by direct comparison that the two different representations of the symbol of the discrete operator $\tilde{\mathscr{D}}_{1,h}^{(2M)}$, given in equations (4.9) and (4.10), with the coefficients λ_{2p-1}^{2M} and γ_{2p-1} as defined in (4.6) and (4.11), respectively, are equivalent for all $M \in \mathbb{N}$.

TABLE 1 *The first four coefficients* γ_{2p-1}

γ_1	γ_3	γ_5	γ_7
1	$\frac{1}{6}$	$\frac{3}{40}$	$\frac{5}{112}$

THEOREM 4.9 $\forall\, M \in \mathbb{N}$, M finite we have

$$\mathscr{F}\left(\tilde{\mathscr{D}}_{1,h}^{(2M)}\right) = \frac{2\mathrm{i}}{h}\sum_{j=1}^{M}\frac{\lambda_{2j-1}^{2M}}{2j-1}\sin\left((2j-1)kh/2\right) = \frac{2\mathrm{i}}{h}\sum_{p=1}^{M}\gamma_{2p-1}\sin^{2p-1}(kh/2). \tag{4.18}$$

Proof. Letting $K := kh/2$, we have, for integers $1 \leqslant j \leqslant M$, the identity

$$\sin\left((2j-1)K\right) = (-1)^{j-1}T_{2j-1}\left(\sin(K)\right), \tag{4.19}$$

where T_{2j-1} are the Chebyshev polynomials of degree $2j-1$. Using properties of these polynomials we can rewrite the right-hand side of (4.19) as

$$\sin\left((2j-1)K\right) = \sum_{p=1}^{j}\alpha_p^j\sin^{2p-1}(K), \tag{4.20}$$

where for $1 \leqslant p \leqslant j$, the coefficients α_p^j in equation (4.20) are given as

$$\alpha_p^j = (-1)^{2j-p-1}\left(\frac{2j-1}{j+p-1}\right)\left(\frac{(j+p-1)!}{(j-p)!}\right)\frac{2^{2p-2}}{(2p-1)!}. \tag{4.21}$$

Substituting (4.20) into the representation (4.9) of the symbol of the operator $\tilde{\mathscr{D}}_{1,h}^{(2M)}$ we have

$$\mathscr{F}\left(\tilde{\mathscr{D}}_{1,h}^{(2M)}\right) = \frac{2\mathrm{i}}{h}\sum_{j=1}^{M}\frac{\lambda_{2j-1}^{2M}}{2j-1}\sin\left((2j-1)K\right) = \frac{2\mathrm{i}}{h}\sum_{j=1}^{M}\frac{\lambda_{2j-1}^{2M}}{2j-1}\sum_{p=1}^{j}\alpha_p^j\sin^{2p-1}(K).$$

Rearranging terms we have

$$\mathscr{F}\left(\tilde{\mathscr{D}}_{1,h}^{(2M)}\right) = \frac{2\mathrm{i}}{h}\sum_{p=1}^{M}\left(\sum_{j=p}^{M}\frac{\lambda_{2j-1}^{2M}}{2j-1}\alpha_p^j\right)\sin^{2p-1}(K). \tag{4.22}$$

Using the formulae (4.6) and (4.21) the coefficients in the expansion (4.22) can be written out as

$$\sum_{j=p}^{M}\frac{\lambda_{2j-1}^{2M}}{2j-1}\alpha_p^j = \sum_{j=p}^{M}\frac{(-1)^{3j-p-2}(j+p-2)![(2M-1)!!]^2 2^{2p-1}}{(2p-1)!(j-p)!(2j-1)(2M-2j)!!(2M+2j-2)!!}. \tag{4.23}$$

Changing the summation index to $k = j-p$ in (4.23), and simplifying terms using the property of the double factorial, $(2n)!! = 2^n n!$, we get

$$\sum_{j=p}^{M}\frac{\lambda_{2j-1}^{2M}}{2j-1}\alpha_p^j = \frac{[(2M-1)!!]^2 2^{2p}}{2^{2M}(2p-1)!}\sum_{k=0}^{M-p}\frac{(-1)^k(2p+k-2)!}{k!(2k+2p-1)(M-p-k)!(M+k+p-1)!}. \tag{4.24}$$

Using representations in terms of hypergeometric functions (verifiable via computer algebra software such as MAPLE) and employing the following identities for $n \in \mathbb{N}$:

$$\Gamma(n+1) = n\Gamma(n); \quad \Gamma\left(n+\frac{1}{2}\right) = \frac{(2n-1)!!\sqrt{\pi}}{2^n}, \tag{4.25}$$

the summation in (4.24) reduces to

$$\sum_{j=p}^{M} \frac{\lambda_{2j-1}^{2M}}{2j-1} \alpha_p^j = \frac{[(2M-1)!!]^2 2^{2p}}{2^{2M}(2p-1)!} \frac{\left[\Gamma\left(p-\frac{1}{2}\right)\right]^2}{4\left[\Gamma\left(M+\frac{1}{2}\right)\right]^2} = \frac{[(2p-3)!!]^2}{(2p-1)!} = \gamma_{2p-1}, \text{ as given in (4.11).} \tag{4.26}$$

Thus, using (4.26) in (4.22), we finally get the result (4.18). □

REMARK 4.10 The formula (4.9), Theorem 4.4 and Theorem 4.9 also apply to the symbol, $\mathscr{F}\left(\mathscr{D}_{1,h}^{(2M)}\right)$, of the operator $\mathscr{D}_{1,h}^{(2M)}$, as defined in equation (4.5).

5. High-order numerical methods for dispersive media

In this section we construct a family of finite difference schemes for Maxwell's equations in Debye and Lorentz dispersive media in one dimension. These schemes are based on the discrete higher-order ($2M$, $M \in \mathbb{N}$) approximations to the first-order operator that were constructed in Section 4. For the time discretization, we employ the standard leap frog scheme that is second-order accurate in time. We will denote the resulting schemes as $(2, 2M)$ schemes. When $M = 1$, the corresponding $(2, 2)$ schemes are extensions of the famous Yee scheme or FDTD scheme for Maxwell's equations in dispersive media.

Let us denote the time step by $\Delta t > 0$ and the spatial mesh step size by $\Delta z > 0$. The nodes of the primary spatial mesh will be denoted by $z_j = j\Delta z$ where $j \in \mathbb{Z}$, while the nodes of the dual spatial mesh will be denoted by $z_{j+\frac{1}{2}} = \left(j+\frac{1}{2}\right)\Delta z$ where $j \in \mathbb{Z}$. The nodes of the primary temporal mesh will be denoted by $t^n = n\Delta t$ where $n \in \mathbb{N}$, while the nodes of the dual temporal mesh will be denoted by $t^{n+\frac{1}{2}} = \left(n+\frac{1}{2}\right)\Delta t$ where $n \in \mathbb{N}$. The discrete solution will be computed at these spatial and temporal nodes (either both primary or both dual) in the space–time mesh. For any field variable $V(t, z)$, we denote the approximation of $V(t^n, z_j)$ by V_j^n on the primary space–time mesh and the approximation of $V\left(t^{n+\frac{1}{2}}, z_{j+\frac{1}{2}}\right)$ by $V_{j+\frac{1}{2}}^{n+\frac{1}{2}}$ on the dual space–time mesh.

With the above notation, the $(2, 2M)$ discretized schemes for Maxwell's equations (3.2) in one dimension are

$$\frac{B_{j+\frac{1}{2}}^{n+\frac{1}{2}} - B_{j+\frac{1}{2}}^{n-\frac{1}{2}}}{\Delta t} = \sum_{p=1}^{M} \frac{\lambda_{2p-1}^{2M}}{2p-1} \left(\frac{E_{j+p}^n - E_{j-p+1}^n}{\Delta z} \right), \tag{5.1a}$$

$$\frac{D_j^{n+1} - D_j^n}{\Delta t} = \frac{1}{\mu_0} \sum_{p=1}^{M} \frac{\lambda_{2p-1}^{2M}}{2p-1} \left(\frac{B_{j+p-\frac{1}{2}}^{n+\frac{1}{2}} - B_{j-p+\frac{1}{2}}^{n+\frac{1}{2}}}{\Delta z} \right), \tag{5.1b}$$

where λ_{2p-1}^{2M} is defined in (4.6). Alternatively, discretizing (3.2a) and (3.3), we have the discrete system given by equation (5.1a) and the following equation:

$$\epsilon_0 \epsilon_\infty \frac{E_j^{n+1} - E_j^n}{\Delta t} = \frac{1}{\mu_0} \sum_{p=1}^{M} \frac{\lambda_{2p-1}^{2M}}{2p-1} \left(\frac{B_{j+p-\frac{1}{2}}^{n+\frac{1}{2}} - B_{j-p+\frac{1}{2}}^{n+\frac{1}{2}}}{\Delta z} \right) - \frac{P_j^{n+1} - P_j^n}{\Delta t}. \tag{5.2}$$

In (5.1b) (respectively, (5.2)), the electric flux density D (respectively, the polarization P) will be determined by the appropriate polarization model.

5.1 $(2, 2M)$ *numerical methods for Debye media*

For Debye media we add the discretized (in time) version of the equation (2.3) given as

$$\epsilon_0\epsilon_\infty\tau\frac{E_j^{n+1}-E_j^n}{\Delta t}+\epsilon_0\epsilon_s\frac{E_j^{n+1}+E_j^n}{2}=\tau\frac{D_j^{n+1}-D_j^n}{\Delta t}+\frac{D_j^{n+1}+D_j^n}{2} \tag{5.3}$$

to the system defined in (5.1a) and (5.1b).

5.2 $(2, 2M)$ *numerical methods for Lorentz media*

For Lorentz media we obtain two types of discretized $(2, 2M)$ methods, based on the second-order differential equation for E in (2.5) or based on the discretization of the system of first-order equations for the variables P and J in (2.6).

5.2.1 $(2, 2M)$ *JHT schemes for Lorentz media.* One set of $(2, 2M)$ schemes for Lorentz media is constructed by adding the time discretized version of the second-order differential equation for E in (2.5) given as

$$\begin{aligned}\epsilon_0\epsilon_\infty\frac{E_j^{n+1}-2E_j^n+E_j^{n-1}}{\Delta t^2}+\nu\epsilon_0\epsilon_\infty\left(\frac{E_j^{n+1}-E_j^{n-1}}{2\Delta t}\right)+\epsilon_0\epsilon_s\omega_0^2\left(\frac{E_j^{n+1}+E_j^{n-1}}{2}\right)\\ =\frac{D_j^{n+1}-2D_j^n+D_j^{n-1}}{\Delta t^2}+\nu\left(\frac{D_j^{n+1}-D_j^{n-1}}{2\Delta t}\right)+\omega_0^2\left(\frac{D_j^{n+1}+D_j^{n-1}}{2}\right)\end{aligned} \tag{5.4}$$

to the discretized Maxwell equations in (5.1a) and (5.1b). We will denote such schemes as $(2, 2M)$ JHT schemes after a similar $(2, 2)$ scheme considered in Joseph *et al*. (1991).

5.2.2 $(2, 2M)$ *KF schemes for Lorentz media.* A second set of $(2, 2M)$ schemes for Lorentz media is constructed by adding the second-order in time discretization of the system of first-order equations for the variables P and J, in equations (2.6), given as

$$\frac{P_j^{n+1}-P_j^n}{\Delta t}=\frac{J_j^{n+1}+J_j^n}{2}, \tag{5.5}$$

$$\frac{J_j^{n+1}-J_j^n}{\Delta t}=-\nu\frac{J_j^{n+1}+J_j^n}{2}+\omega_p^2\epsilon_0\frac{E_j^{n+1}+E_j^n}{2}-\omega_0^2\frac{P_j^{n+1}+P_j^n}{2} \tag{5.6}$$

to the discretized system of Maxwell's equations in (5.1a) and (5.2). We will denote such schemes as $(2, 2M)$ KF schemes after a similar $(2, 2)$ scheme considered in Kashiwa & Fukai (1990).

6. Stability analysis

To determine stability conditions we use von Neumann analysis that allows us to localize roots of certain classes of polynomials (see, e.g., Bidégaray-Fesquet, 2008). We follow the approach in Bidégaray-Fesquet (2008) in which the author derives stability conditions for the (2, 2) (Yee) schemes applied to Debye and Lorentz dispersive media. This analysis is based on properties of Schur and von Neumann polynomials.

Stability conditions for the general $(2, 2M)$ schemes are made possible by the results presented in Section 4 in which finite difference approximations of the first-order derivative operator are obtained as a result of the truncation of an appropriate series expansion of the symbol of this operator.

In performing the von Neumann analysis for the $(2, 2M)$ schemes we show that the resulting amplification matrices retain the same structure as in the (2, 2) schemes in Bidégaray-Fesquet (2008), albeit with a generalized definition of the parameter q in Bidégaray-Fesquet (2008). We also note that these polynomials have the same structure as those derived for the (2, 2) schemes in Petropoulos (1994). This affords a complete stability analysis for the general case, as results from Bidégaray-Fesquet (2008) can be used directly for the generalized parameter q as we show below.

We refer the reader to Bidégaray-Fesquet (2008) for a description of von Neumann analysis and for the major theorems regarding properties of Schur and von Neumann polynomials that aid in the construction of stability criteria for the various finite difference schemes.

6.1 *Stability analysis for* $(2, 2M)$ *schemes for Debye media*

We consider the $(2, 2M)$ scheme for discretizing Maxwell's equations coupled with the Debye polarization model presented in the form of equations (5.1a), (5.1b) and (5.3). We rewrite these equations using the (modified) variables $c_\infty B_{j+\frac{1}{2}}^{n-\frac{1}{2}}$, E_j^n and $\frac{1}{\epsilon_0\epsilon_\infty} D_j^n$ to obtain the modified system

$(2, 2M)$ Debye:

$$c_\infty B_{j+\frac{1}{2}}^{n+\frac{1}{2}} = c_\infty B_{j+\frac{1}{2}}^{n-\frac{1}{2}} + \eta \sum_{p=1}^{M} \frac{\lambda_{2p-1}^{2M}}{2p-1} \left(E_{j+p}^n - E_{j-p+1}^n \right), \tag{6.1a}$$

$$E_j^{n+1} = \left(\frac{2 - h_\tau \epsilon_q}{2 + h_\tau \epsilon_q} \right) E_j^n + \left(\frac{2 + h_\tau}{2 + h_\tau \epsilon_q} \right) \frac{1}{\epsilon_0\epsilon_\infty} D_j^{n+1} - \left(\frac{2 - h_\tau}{2 + h_\tau \epsilon_q} \right) \frac{1}{\epsilon_0\epsilon_\infty} D_j^n, \tag{6.1b}$$

$$\frac{1}{\epsilon_0\epsilon_\infty} D_j^{n+1} = \frac{1}{\epsilon_0\epsilon_\infty} D_j^n + \eta c_\infty \sum_{p=1}^{M} \frac{\lambda_{2p-1}^{2M}}{2p-1} \left(B_{j+p-\frac{1}{2}}^{n+\frac{1}{2}} - B_{j-p+\frac{1}{2}}^{n+\frac{1}{2}} \right). \tag{6.1c}$$

In equations (6.1a)–(6.1c) the parameter $c_\infty^2 := 1/(\epsilon_0\mu_0\epsilon_\infty) = c_0^2/\epsilon_\infty$ and the parameter $\eta := (c_\infty \Delta t)/\Delta z$, where c_0 is the speed of light in vacuum, and c_∞ is the maximum speed of light in the Debye medium. The parameter η is the Courant (stability) number. The parameters h_τ and ϵ_q are defined as

$$h_\tau := \Delta t/\tau, \quad \epsilon_q := \epsilon_s/\epsilon_\infty. \tag{6.2}$$

We assume here that $\epsilon_s > \epsilon_\infty$, i.e., $\epsilon_q > 1$ and $\tau > 0$, which is the case for most practical applications.

All the models that we deal with are linear. Thus, we can analyse the models in the frequency domain. We look for plane wave solutions of (6.1) as numerically evaluated at the discrete space–time point (t^n, z_j) or $(t^{n+1/2}, z_{j+1/2})$. We assume a spatial dependence of the form

$$B_{j+\frac{1}{2}}^{n+\frac{1}{2}} = \hat{B}^{n+\frac{1}{2}}(k)\mathrm{e}^{\mathrm{i}kz_{j+\frac{1}{2}}}, \quad E_j^n = \hat{E}^n(k)\mathrm{e}^{\mathrm{i}kz_j}, \quad D_j^n = \hat{D}^n(k)\mathrm{e}^{\mathrm{i}kz_j}, \tag{6.3}$$

in the field quantities, with k defined to be the wave number. (Equivalently, we can apply the discrete Fourier transform in space to the discrete equations (6.1).) Define the vector $\mathbf{U}^n := \left[c_\infty \hat{B}^{n-\frac{1}{2}}, \hat{E}^n, \frac{1}{\epsilon_0\epsilon_\infty}\hat{D}^n\right]^{\mathrm{T}}$. Substituting the forms (6.3) into the higher-order schemes (6.1) and cancelling out common terms we obtain the system $\mathbf{U}^{n+1} = \mathscr{A}\mathbf{U}^n$, where the amplification matrix $\mathscr{A}$ is

$$\mathscr{A} = \begin{bmatrix} 1 & -\sigma & 0 \\ -\left(\frac{2+h_\tau}{2+h_\tau\epsilon_q}\right)\sigma & \left(\frac{2(1-q)-h_\tau(\epsilon_q+q)}{2+h_\tau\epsilon_q}\right) & \left(\frac{2h_\tau}{2+h_\tau\epsilon_q}\right) \\ -\sigma & -q & 1 \end{bmatrix}, \tag{6.4}$$

with the parameter σ defined as

$$\sigma := -2\mathrm{i}\eta \sum_{p=1}^{M} \gamma_{2p-1} \sin^{2p-1}\left(\frac{k\,\Delta z}{2}\right), \tag{6.5}$$

and $\sigma^* = -\sigma$ is the complex conjugate of σ. The parameter q is defined to be

$$q := |\sigma|^2 = \sigma\sigma^* = 4\eta^2 \left(\sum_{p=1}^{M} \gamma_{2p-1} \sin^{2p-1}\left(\frac{k\,\Delta z}{2}\right)\right)^2. \tag{6.6}$$

Here, we are using the equivalence between the two different representations of the symbols of the discrete (spatial) operators $\tilde{\mathscr{D}}_{1,h}^{(2M)}$ and $\mathscr{D}_{1,h}^{(2M)}$ of order $2M$, given in Theorem 4.4 (see Remark 4.10). This is reflected in the presence of the term σ, as defined in (6.5), in the amplification matrix given in (6.4).

The characteristic polynomial is given by

$$\begin{aligned} P_{(2,2M)}^{\mathrm{D}}(\zeta) = \zeta^3 &+ \left(\frac{q\epsilon_\infty(2+h_\tau) - (6\epsilon_\infty + h_\tau\epsilon_{\mathrm{s}})}{2\epsilon_\infty + h_\tau\epsilon_{\mathrm{s}}}\right)\zeta^2 \\ &+ \left(\frac{q\epsilon_\infty(h_\tau - 2) + (6\epsilon_\infty - h_\tau\epsilon_{\mathrm{s}})}{2\epsilon_\infty + h_\tau\epsilon_{\mathrm{s}}}\right)\zeta - \left(\frac{2\epsilon_\infty - h_\tau\epsilon_{\mathrm{s}}}{2\epsilon_\infty + h_\tau\epsilon_{\mathrm{s}}}\right). \end{aligned} \tag{6.7}$$

We note that for the case $M = 1$, the characteristic polynomial (6.7) is the same as that derived in Bidégaray-Fesquet (2008) as well as that derived in Petropoulos (1994). In Bidégaray-Fesquet (2008) stability analysis was performed for the (2, 2) schemes only, and thus q was defined as $q = 4\eta^2 \sin^2\left(\frac{kh}{2}\right)$ ($M = 1$ in equation (6.6)). The representation (4.10) for the symbols of $\tilde{\mathscr{D}}_{1,h}^{(2M)}$ and $\mathscr{D}_{1,h}^{(2M)}$ allows us to retain the same compact form of the (2, 2) characteristic polynomial for the general $(2, 2M)$ schemes by using the generalized definition (6.6) of the parameter q, which depends on M.

Now, using the results of the von Neumann stability analysis performed in Bidégaray-Fesquet (2008), we can generalize the stability analysis to the $(2, 2M)$ schemes. From the assumption $\epsilon_s > \epsilon_\infty$, a necessary and sufficient stability condition for the $(2, 2M)$ scheme in (6.1) is that $q \in (0, 4)$, for all wave numbers, k (see Bidégaray-Fesquet, 2008), i.e.,

$$4\eta^2 \left(\sum_{p=1}^{M} \gamma_{2p-1} \sin^{2p-1} \left(\frac{k\,\Delta z}{2} \right) \right)^2 < 4 \quad \forall\, k, \tag{6.8}$$

which implies that

$$\eta \left(\sum_{p=1}^{M} \gamma_{2p-1} \right) < 1 \Longleftrightarrow \Delta t < \frac{\Delta z}{\left(\sum_{p=1}^{M} \frac{[(2p-3)!!]^2}{(2p-1)!} \right) c_\infty}. \tag{6.9}$$

In the limiting case (as $M \to \infty$) we may evaluate the infinite series using Lemma 4.8. Therefore,

$$M = \infty, \quad \eta \left(\frac{\pi}{2} \right) < 1 \Longleftrightarrow \Delta t < \frac{2\,\Delta z}{\pi\, c_\infty}. \tag{6.10}$$

The positivity of the coefficients γ_{2p-1} gives that the constraint on Δt in (6.10) is a lower bound on all constraints for any $M \in \mathbb{N}$. Therefore, this constraint guarantees stability for all orders.

6.2 *Numerical dissipation for* $(2, 2M)$ *schemes for Debye media*

While the stability criteria (6.9) give conditions for which the finite difference methods of various orders are stable, they do not give any insight into the amount of error, specifically, numerical dissipation error that may be exhibited by a particular order of method. We follow the procedures in Petropoulos (1994) and Banks *et al*. (2009) to produce plots of the numerical (artificial) dissipation for the scheme (6.1). To generate these plots we have assumed the following values of the physical parameters:

$$\epsilon_\infty = 1, \quad \epsilon_s = 78.2, \quad \tau = 8.1 \times 10^{-12}\ \text{s}. \tag{6.11}$$

These are appropriate constants for modelling water and are representative of a large class of Debye type materials (see, e.g., Banks *et al*., 2000). In order to resolve all the time scales the time step Δt is determined by the choice of h_τ and the physical parameter τ. In the left plot of Fig. 1, we graph the absolute value of the largest root, ζ, of (6.7), as a function of $k\,\Delta z$, using $h_\tau = 0.1$ for the finite-difference scheme (6.1) of (spatial) orders $2M = 2, 4, 6, 8$ and the limiting ($M = \infty$) case with η set to the maximum stable value for each order, given in (6.9) for finite M, and in (6.10) for $M = \infty$. In the right plot, we fix η to the maximum stable value for the limiting ($M = \infty$) case (i.e., each method uses the same value of η and that value is the largest for which all methods are guaranteed stable). Note that in the limit as $h_\tau \to 0$ in (6.7), we have that $\max|\zeta| = 1$.

We can interpret $k\,\Delta z$ as the wave number if Δz is fixed or as the inverse of the number of points per wavelength (N_{ppw}) if k is fixed. Using the latter interpretation it is reasonable to assume that in most practical implementations $k\,\Delta z \leqslant 1$ for most wave numbers of interest in the problem. We note that while the left plot suggests that the infinite-order method has the least numerical dissipation (maximum complex time eigenvalue closest to 1), this is mostly a consequence of the severe restriction on η. It is clear in the right plot that, with all material and discretization parameters held fixed at equivalent values

for all orders of the finite difference method, the second-order method exhibits the least numerical dissipation for most wave numbers.

For each of the curves in both plots of Fig. 1, the maximum numerical dissipation error (formally defined here to be 1 minus the minimum value of the curve) is unacceptably high with a value $(1-\max|\zeta|)$ between 0.1 and 0.2. The numerical dissipation error of the schemes can be reduced by decreasing h_τ. Note that we are assuming the time step Δt is determined by the choice of h_τ and the (fixed and known) physical parameter τ. The left and right plots of Fig. 2 depict $\max|\zeta|$ using $h_\tau = 0.01$ (note the difference in axes). We see that the maximum numerical dissipation error decreases by an order of magnitude (to 0.02). We also note that, as seen in the right plot, the methods of different orders are virtually indistinguishable at this discretization level.

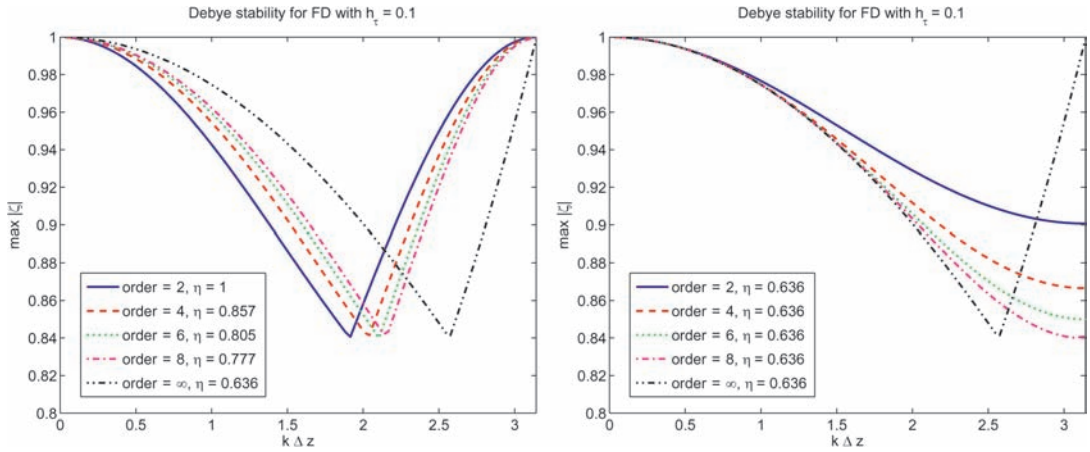

FIG. 1. (Left) $\max|\zeta|$ versus $k\,\Delta z$ using $h_\tau = 0.1$ for the schemes (6.1) of orders $2M = 2, 4, 6, 8$ and the limiting ($M = \infty$) case with η set to the maximum stable value for the order, given in (6.9) for finite M, and in (6.10) for $M = \infty$. (Right) η fixed at the maximum stable value for the limiting ($M = \infty$) case, given in (6.10).

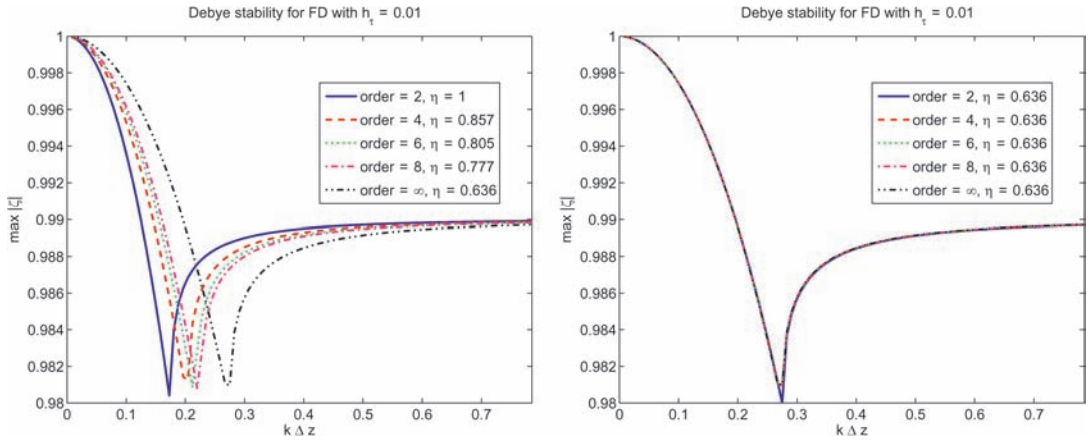

FIG. 2. Left and right plots are similar to corresponding plots of Fig. 1 except here $h_\tau = 0.01$. Note the change in axes from those of Fig. 1.

6.3 *Stability analysis for* $(2, 2M)$ *KF schemes for Lorentz media*

We consider the $(2, 2M)$ scheme for discretizing Maxwell's equations, coupled with the discretization of the Lorentz polarization model, presented in the form of equations (5.1a) and (5.2) along with equations (5.5) and (5.6). We rewrite the scheme using the (modified) variables $c_\infty B^{n-\frac{1}{2}}_{j+\frac{1}{2}}$, E^n_j, $\frac{1}{\epsilon_0\epsilon_\infty}P^n_j$ and $\frac{\Delta t}{\epsilon_0\epsilon_\infty}J^n_j$ to get the modified system

$(2, 2M)$ KF:

$$c_\infty B^{n+\frac{1}{2}}_{j+\frac{1}{2}} = c_\infty B^{n-\frac{1}{2}}_{j+\frac{1}{2}} + \eta \sum_{p=1}^{M} \frac{\lambda^{2M}_{2p-1}}{2p-1}\left(E^n_{j+p} - E^n_{j-p+1}\right), \tag{6.12a}$$

$$E^{n+1}_j = E^n_j + \eta c_\infty \sum_{p=1}^{M} \frac{\lambda^{2M}_{2p-1}}{2p-1}\left(B^{n+\frac{1}{2}}_{j+p-\frac{1}{2}} - B^{n+\frac{1}{2}}_{j-p+\frac{1}{2}}\right) - \frac{1}{\epsilon_0\epsilon_\infty}\left(P^{n+1}_j - P^n_j\right), \tag{6.12b}$$

$$P^{n+1}_j = P^n_j + \frac{\Delta t}{2}\left(J^{n+1}_j + J^n_j\right), \tag{6.12c}$$

$$J^{n+1}_j = J^n_j + \frac{\Delta t}{2} t\left(\omega_p^2\epsilon_0\left(E^{n+1}_j + E^n_j\right) - \nu\left(J^{n+1}_j + J^n_j\right) - \omega_0^2\left(P^{n+1}_j + P^n_j\right)\right). \tag{6.12d}$$

As done for Debye media, we look for plane wave solutions of (6.12) as numerically evaluated at the discrete space–time points (t^n, x_j) or $(t^{n+1/2}, z_{j+1/2})$. We assume a spatial dependence of the form

$$B^{n+\frac{1}{2}}_{j+\frac{1}{2}} = \hat{B}^{n+\frac{1}{2}}(k)\mathrm{e}^{\mathrm{i}kz_{j+\frac{1}{2}}}, \quad E^n_j = \hat{E}^n(k)\mathrm{e}^{\mathrm{i}kz_j}, \quad P^n_j = \hat{P}^n(k)\mathrm{e}^{\mathrm{i}kz_j}, \quad J^n_j = \hat{J}^n(k)\mathrm{e}^{\mathrm{i}kz_j},$$

where k is the wave number. Define the vector $\mathbf{U}^n := \left[c_\infty\hat{B}^{n-\frac{1}{2}}, \hat{E}^n, \frac{1}{\epsilon_0\epsilon_\infty}\hat{P}^n, \frac{\Delta t}{\epsilon_0\epsilon_\infty}\hat{J}^n\right]^{\mathrm{T}}$. Proceeding as in the Debye case we obtain the system $\mathbf{U}^{n+1} = \mathscr{A}\mathbf{U}^n$, where the amplification matrix $\mathscr{A}$ for this method is given by

$$\mathscr{A} = \begin{bmatrix} 1 & -\sigma & 0 & 0 \\ \left(\frac{\pi^2h_0^2(\epsilon_q-1)}{\theta_+} - 1\right)\sigma & (1-q) - \frac{(2-q)(\epsilon_q-1)\pi^2h_0^2}{\theta_+} & \frac{2\pi^2h_0^2}{\theta_+} & \frac{-1}{\theta_+} \\ -\frac{\pi^2h_0^2(\epsilon_q-1)}{\theta_+}\sigma & \frac{(2-q)(\epsilon_q-1)\pi^2h_0^2}{\theta_+} & 1 - \frac{2\pi^2h_0^2}{\theta_+} & \frac{1}{\theta_+} \\ -\frac{2\pi^2h_0^2(\epsilon_q-1)}{\theta_+}\sigma & \frac{2(2-q)(\epsilon_q-1)\pi^2h_0^2}{\theta_+} & \frac{-4\pi^2h_0^2}{\theta_+} & \frac{2-\theta_+}{\theta_+} \end{bmatrix},$$

where the parameters h_0 and θ_+ are defined as

$$h_0 := (\omega_0\Delta t)/(2\pi), \tag{6.13}$$

$$\theta_+ := 1 + h_\nu/2 + \pi^2h_0^2\epsilon_q, \tag{6.14}$$

and the parameters σ and q are as given in (6.5) and (6.6), respectively. The parameter ϵ_q is defined in (6.2), and the parameter h_ν is defined as

$$h_\nu := \nu\, \Delta t. \tag{6.15}$$

As in the case of the Debye model, the characteristic polynomial for the $(2, 2M)$ KF scheme retains the same structure as in Petropoulos (1994) for the case $M = 1$ with the generalized definition of the parameter q (defined in (6.6)) for arbitrary even order $2M$:

$$P^{\mathrm{KF}}_{(2,2M)}(\zeta) = \zeta^4 + \zeta^3 \left(\frac{\theta_3 q + \theta_3'}{\theta_0}\right) + \zeta^2 \left(\frac{\theta_2 q + \theta_2'}{\theta_0}\right) + \zeta \left(\frac{\theta_1 q + \theta_1'}{\theta_0}\right) + \frac{\theta_0'}{\theta_0}, \tag{6.16}$$

where, the coefficients in (6.16) are defined as

$$\begin{aligned}
&\theta_3 = 2 + h_\nu + 2\pi^2 h_0^2, \quad \theta_3' = -8 - 2h_\nu,\\
&\theta_2 = 4\pi^2 h_0^2 - 4, \quad \theta_2' = -4\pi^2 h_0^2 \epsilon_q + 12,\\
&\theta_1 = 2 + 2\pi^2 h_0^2 - h_\nu, \quad \theta_1' = -8 + 2h_\nu,\\
&\theta_0 = 2 + h_\nu + 2\pi^2 h_0^2 \epsilon_q, \quad \theta_0' = 2 - h_\nu + 2\pi^2 h_0^2 \epsilon_q.
\end{aligned} \tag{6.17}$$

Again, assuming that $\epsilon_{\mathrm{s}} > \epsilon_\infty$, i.e., $\epsilon_q > 1$, and $\nu > 0$, and applying the results of the von Neumann analysis conducted in Bidégaray-Fesquet (2008) gives us the stability condition: $q \in (0, 4)$ for all wave numbers, k, i.e.,

$$4\eta^2 \left(\sum_{p=1}^{M} \gamma_{2p-1} \sin^{2p-1}\left(\frac{kh}{2}\right)\right)^2 < 4 \quad \forall\, k, \tag{6.18}$$

which implies that

$$M < \infty, \quad \eta \left(\sum_{p=1}^{M} \gamma_{2p-1}\right) < 1 \Longleftrightarrow \Delta t < \frac{\Delta z}{\left(\sum_{p=1}^{M} \frac{[(2p-3)!!]^2}{(2p-1)!}\right) c_\infty}, \tag{6.19a}$$

$$M = \infty, \quad \eta \left(\frac{\pi}{2}\right) < 1 \Longleftrightarrow \Delta t < \frac{2\Delta z}{\pi\, c_\infty}. \tag{6.19b}$$

Again, the positivity of the coefficients γ_{2p-1} gives that the constraint in (6.19b) guarantees stability for all orders M.

6.4 *Numerical dissipation for* $(2, 2M)$ *KF schemes for Lorentz media*

To generate the plots in this section we have used the representative Lorentz model material parameters chosen by Brillouin (1960),

$$\epsilon_\infty = 1, \quad \epsilon_{\mathrm{s}} = 2.25, \quad \nu = 0.56 \times 10^{16}\ \mathrm{s}^{-1}, \quad \omega_0 = 4 \times 10^{16}\ \mathrm{rad/s}. \tag{6.20}$$

These are typical values that are used in the study of physical optics and are representative of a highly absorptive and dispersive medium (see Banks *et al.*, 2009). For the Lorentz medium all time scales must be properly resolved. Therefore, the time step Δt is determined by the choice of either h_ν (defined in (6.15)) or h_0 (defined in (6.13)), whichever is most restrictive. For the parameter values chosen in (6.20), since $\frac{2\pi}{\omega_0} < \frac{1}{\nu}$, h_0 is more restrictive than h_ν.

In the left plot of Fig. 3, we graph the absolute value of the largest root, ζ, of (6.16), as a function of $k\Delta z$, using $h_0 = 0.1$ for the $(2, 2M)$ KF schemes of (spatial) orders $2M = 2, 4, 6, 8$, given in equations (6.12), and the limiting ($M = \infty$) case with η set to the maximum stable value for each order, as given in (6.19). In the right plot, we fix η to the maximum stable value for the limiting (order $= \infty$) case (i.e., each method uses the same value of η and that value is the largest for which all methods are guaranteed stable).

As in the Debye case, the left plot suggests that the infinite-order method has the least numerical dissipation for small values of $k\Delta z$, however, this is again mostly a consequence of the severe restriction on η. The right plot demonstrates that for all material and discretization parameters held fixed at equivalent values for all orders of the $(2, 2M)$ KF schemes, the second-order method has the least numerical dissipation for small $k\Delta z$, albeit only by a small amount. Refining the temporal discretization, as in the Debye analysis, we see that the methods of various orders conform as depicted in Fig. 4 (see also Bokil & Gibson, 2010). It is interesting to note that the maximum numerical dissipation error (again, defined here to be 1 minus the minimum value of the curve) for the $(2, 2M)$ KF schemes (and the assumed parameter values) is approximately $0.2h_0$, and the minimizer of the curves moves to the left by an order of magnitude as h_0 is likewise decreased. However, unlike in the Debye case, the maximum numerical dissipation error goes to 0 much faster as $k\Delta z$ increases, rather than levelling to half of the maximum dissipation error (before eventually going to zero). This is a positive property in the case of broad band signals.

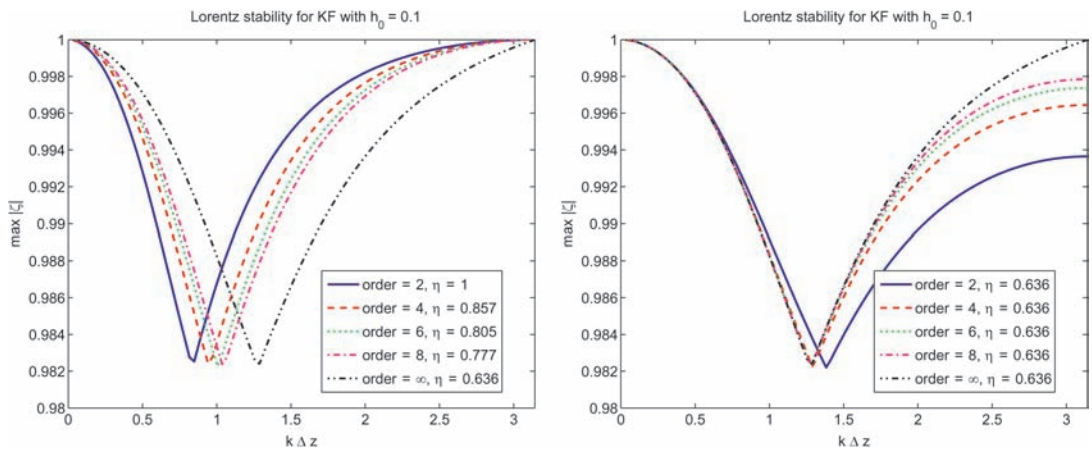

FIG. 3. (Left) $\max|\zeta|$ versus $k\Delta z$ using $h_0 = 0.1$ for the $(2, 2M)$ KF schemes of orders $2M = 2, 4, 6, 8$, given in equations (6.12), and the limiting ($M = \infty$) case with η set to the maximum stable value for the order, as given in (6.19). (Right) is with η fixed at the maximum stable value for the limiting ($M = \infty$) case.

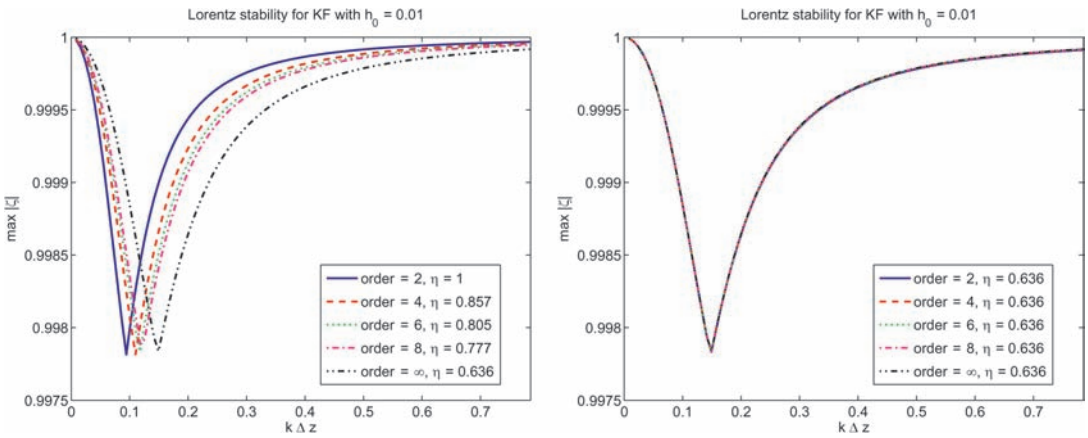

FIG. 4. Left and right plots are similar to corresponding plots in Fig. 3 except here $h_0 = 0.01$. Note the change in axes from Fig. 3.

6.5 *Stability analysis for* $(2, 2M)$ *JHT schemes for Lorentz media*

Finally, we consider the $(2, 2M)$ schemes for discretizing Maxwell's equations coupled with the discretization of the Lorentz polarization model presented in equations (5.1a) and (5.1b) along with equation (5.4). Using the (modified) variables $c_\infty B^{n-\frac{1}{2}}_{j+\frac{1}{2}}$, E^n_j, E^{n-1}_j and $\frac{1}{\epsilon_0\epsilon_\infty} D^n_j$ we rewrite this system as

$(2, 2M)$ JHT:

$$c_\infty B^{n+\frac{1}{2}}_{j+\frac{1}{2}} = c_\infty B^{n-\frac{1}{2}}_{j+\frac{1}{2}} + \eta \sum_{p=1}^{M} \frac{\lambda^{2M}_{2p-1}}{2p-1} \left(E^n_{j+p} - E^n_{j-p+1} \right), \tag{6.21a}$$

$$\frac{1}{\epsilon_0\epsilon_\infty} D^{n+1}_j = \frac{1}{\epsilon_0\epsilon_\infty} D^n_j + \eta c_\infty \sum_{p=1}^{M} \frac{\lambda^{2M}_{2p-1}}{2p-1} \left(B^{n+\frac{1}{2}}_{j+p-\frac{1}{2}} - B^{n+\frac{1}{2}}_{j-p+\frac{1}{2}} \right), \tag{6.21b}$$

$$\begin{aligned} \frac{\phi_+}{2} E^{n+1}_j &= 2E^n_j - \frac{\phi_-}{2} E^{n-1}_j + \frac{1}{\epsilon_0\epsilon_\infty} \left(D^{n+1}_j - 2D^n_j + D^{n-1}_j \right) \\ &\quad + \frac{h_v}{2} \frac{1}{\epsilon_0\epsilon_\infty} \left(D^{n+1}_j - D^{n-1}_j \right) + 2\pi^2 h_0^2 \frac{1}{\epsilon_0\epsilon_\infty} \left(D^{n+1}_j + D^{n-1}_j \right), \end{aligned} \tag{6.21c}$$

where the parameters ϕ_+ and ϕ_- are defined as

$$\phi_- := 2 - h_v + 4\pi^2 h_0^2 \epsilon_q, \tag{6.22}$$

$$\phi_+ := 2 + h_v + 4\pi^2 h_0^2 \epsilon_q, \tag{6.23}$$

with the parameters ϵ_q, h_v and h_0 as defined in equations (6.2), (6.15) and (6.13), respectively.

We look for plane wave solutions of the equations (6.21) as numerically evaluated at the discrete space–time points (t^n, x_j) or $(t^{n+1/2}, z_{j+1/2})$. We assume a spatial dependence of the form

$$B^{n+\frac{1}{2}}_{j+\frac{1}{2}} = \hat{B}^{n+\frac{1}{2}}(k) \mathrm{e}^{\mathrm{i}kz_{j+\frac{1}{2}}}, \quad E^n_j = \hat{E}^n(k) \mathrm{e}^{\mathrm{i}kz_j}, \quad D^n_j = \hat{D}^n(k) \mathrm{e}^{\mathrm{i}kz_j}. \tag{6.24}$$

Define the vector $\mathbf{U}^n := \left[\mathrm{c}_\infty \hat{B}^{n-\frac{1}{2}}, \hat{E}^n, \hat{E}^{n-1}, \frac{1}{\epsilon_0 \epsilon_\infty}\hat{D}^n\right]$. Proceeding as before, we obtain the system $\mathbf{U}^{n+1} = \mathscr{A}\mathbf{U}^n$, where the amplification matrix $\mathscr{A}$ for this method is given by

$$\mathscr{A} = \begin{bmatrix} 1 & -\sigma & 0 & 0 \\ -\frac{2\sigma h_\nu}{\phi_+} & \frac{2(2-q(1+h_\nu/2+2\pi^2 h_0^2))}{\phi_+} & \frac{-\phi_-}{\phi_+} & \frac{8\pi^2 h_0^2}{\phi_+} \\ 0 & 1 & 0 & 0 \\ -\sigma & -q & 0 & 1 \end{bmatrix}, \tag{6.25}$$

where σ and q are as defined in (6.5) and (6.6), respectively. The characteristic polynomial for the $(2, 2M)$ JHT scheme for the Lorentz model becomes

$$P^{\mathrm{JHT}}_{(2,2M)}(\zeta) = \zeta^4 + \zeta^3\left(\frac{\phi_3 q + \phi_3'}{\phi_+}\right) + \zeta^2\left(\frac{\phi_2 q + \phi_2'}{\phi_+}\right) + \zeta\left(\frac{\phi_1 q + \phi_1'}{\phi_+}\right) + \frac{\phi_-}{\phi_+}, \tag{6.26}$$

where, the coefficients in (6.26) are

$$\begin{aligned} &\phi_3 := 2 + h_\nu + 4\pi^2 h_0^2, \quad \phi_3' := -8 - 2h_\nu - 8\pi^2 h_0^2 \epsilon_q, \\ &\phi_2 := -4, \quad \phi_2' := 8\pi^2 h_0^2 \epsilon_q + 12, \\ &\phi_1 := 2 + 4\pi^2 h_0^2 - h_\nu, \quad \phi_1' := -8 - 2h_\nu - 8\pi^2 h_0^2 \epsilon_q, \end{aligned} \tag{6.27}$$

and ϕ_+ and ϕ_- are as defined in (6.23) and (6.22), respectively. Again, we are able to retain the same structure for the characteristic polynomial as in Petropoulos (1994) (for the case $M = 1$) with the generalized definition of the parameter q (defined in (6.6)) for arbitrary even order $2M$, and it is equivalent to the characteristic polynomial in Bidégaray-Fesquet (2008) for the case $M = 1$.

Further, assuming that $\epsilon_s > \epsilon_\infty$, i.e., $\epsilon_q > 1$, and $\nu > 0$, and applying the results of the von Neumann analysis conducted in Bidégaray-Fesquet (2008) gives us the following stability condition: $q \in (0, 2)$, for all wave numbers, k, i.e.,

$$4\eta^2 \left(\sum_{p=1}^{M} \gamma_{2p-1} \sin^{2p-1}\left(\frac{kh}{2}\right)\right)^2 < 2 \quad \forall\, k. \tag{6.28}$$

Thus, we obtain the stability conditions

$$M < \infty, \quad \eta\left(\sum_{p=1}^{M} \gamma_{2p-1}\right) < \frac{1}{\sqrt{2}} \Longleftrightarrow \Delta t < \frac{\Delta z}{\left(\sum_{p=1}^{M} \frac{[(2p-3)!!]^2}{(2p-1)!}\right)\sqrt{2}c_\infty}, \tag{6.29a}$$

$$M = \infty, \quad \eta\left(\frac{\pi}{2}\right) < \frac{1}{\sqrt{2}} \Longleftrightarrow \Delta t < \frac{\sqrt{2}\,\Delta z}{\pi\ \mathrm{c}_\infty}. \tag{6.29b}$$

Again, the positivity of the coefficients γ_{2p-1} gives that the constraint in (6.29b) guarantees stability for all orders M.

6.6 *Numerical dissipation for* $(2, 2M)$ *JHT schemes for Lorentz media*

To generate the plots in this section we have used the representative Lorentz model material parameters given in (6.20). While quantitatively different the numerical dissipation plots for the $(2, 2M)$ JHT schemes with $h_0 = 0.1$ are qualitatively the same as those for the KF scheme (see Bokil & Gibson, 2010). Although the stability conditions for $(2, 2M)$ JHT schemes are more restrictive, there is no distinct advantage over the (corresponding) $(2, 2M)$ KF schemes with respect to numerical dissipation resulting from enforcing this constraint. The magnitude of the maximum numerical dissipation errors, while slightly less for fixed values of $k\Delta z$, seems to be comparable to those of the (corresponding) $(2, 2M)$ KF schemes. As in the Debye stability analysis, the effect of the order of the method is negligible when considering small discretization parameters (whether h_0 or $k\Delta z$) and holding the value of η fixed.

7. Dispersion analysis

A time-dependent scalar linear PDE with constant coefficients on an unbounded space domain admits plane wave solutions of the form $e^{i(kz-\omega t)}$, where k is the wave number and ω the frequency. The PDE imposes a relation of the form $\omega = \omega(k)$, which is called a dispersion relation. The PDE itself is called dispersive if the speed of propagation of waves depends on the wave number k (or on ω). Finite difference approximations on uniform meshes to the PDEs also admit plane wave solutions of the form $e^{i(k_\Delta j\Delta z-\omega n\Delta t)}$, where k_Δ represents the so-called numerical wave number. Regardless of whether the PDE is dispersive, any finite difference approximation will exhibit spurious dispersion (see, e.g., Trefethen, 1982). The dispersion relation of the numerical method is called a numerical dispersion relation as it is an artifact of the numerical scheme.

As mentioned in Section 1, the models for Debye and Lorentz media have actual physical dispersion that needs to be modelled correctly. In this section we construct the numerical dispersion relations for the $(2, 2M)$ schemes considered in Section 5 for Debye and Lorentz dispersive media. We plot the phase error for all these different methods by using representative values for all the parameters of each model. We follow the approach in Petropoulos (1994) in which dispersion analysis was conducted for the $(2, 2)$ (or Yee) finite difference scheme for Debye and Lorentz media.

7.1 *Debye media*

A plane wave solution of the continuous Debye model (2.3), which is coupled with the Maxwell system (3.2), gives us the following (exact) dispersion relation

$$k_{\mathrm{EX}}^{\mathrm{D}}(\omega) = \frac{\omega}{c}\sqrt{\epsilon_{\mathrm{r}}^{\mathrm{D}}(\omega)}, \quad \epsilon_{\mathrm{r}}^{\mathrm{D}}(\omega) := \frac{\epsilon_{\mathrm{s}}\lambda - \mathrm{i}\omega\epsilon_\infty}{\lambda - \mathrm{i}\omega}. \tag{7.1}$$

In the above, $\epsilon_{\mathrm{r}}^{\mathrm{D}}(\omega)$ is the relative complex permittivity of the Debye medium, $\lambda := 1/\tau$ and ω is the angular frequency.

By considering plane wave solutions for all the discrete variables in the $(2, 2M)$ finite difference schemes for Debye media given in (6.1), we can derive the numerical dispersion relation of this scheme. First, we define the following quantity that relates the order of the method to the resulting numerical wave number $k_{\Delta,M}$

$$K_{\Delta,M}(\omega) := \frac{2}{\Delta z}\sum_{p=1}^{M}\gamma_{2p-1}\sin^{2p-1}\left(\frac{k_{\Delta,M}(\omega)\Delta z}{2}\right), \tag{7.2}$$

where the coefficients γ_{2p-1} are those defined in Theorem 4.4. Thus, the numerical dispersion relations of the $(2, 2M)$ schemes for the Debye model, which implicitly give $k_{\Delta,M} = k^{\mathrm{D}}_{\mathrm{FD},M}$ as a function of discretization parameters and ω, can be succinctly written as

$$K^{\mathrm{D}}_{\mathrm{FD},M}(\omega) = \frac{\omega_\Delta}{c}\sqrt{\epsilon^{\mathrm{D}}_{\mathrm{r,FD}}}, \quad \epsilon^{\mathrm{D}}_{\mathrm{r,FD}} := \frac{\epsilon_{\mathrm{s},\Delta}\lambda_\Delta - \mathrm{i}\omega_\Delta\epsilon_{\infty,\Delta}}{\lambda_\Delta - \mathrm{i}\omega_\Delta}, \tag{7.3}$$

where the parameters

$$\epsilon_{\mathrm{s},\Delta} := \epsilon_{\mathrm{s}}; \quad \epsilon_{\infty,\Delta} := \epsilon_\infty; \quad \lambda_\Delta := \lambda\cos(\omega\Delta t/2) \tag{7.4}$$

are discrete representations of the corresponding continuous model parameters. In addition the parameter ω_Δ, which is a discrete representation of the frequency, is defined as

$$\omega_\Delta := \omega\frac{\sin(\omega\Delta t/2)}{\omega\Delta t/2}. \tag{7.5}$$

We define the phase error $\boldsymbol{\Phi}$ for any method applied to a particular model to be

$$\boldsymbol{\Phi} = \left|\frac{k_{\mathrm{EX}} - k_{\Delta,M}}{k_{\mathrm{EX}}}\right|, \tag{7.6}$$

where the numerical wave number $k_{\Delta,M}$ is implicitly determined by the corresponding dispersion relation and k_{EX} is the exact wave number for the given model. We wish to examine the phase error as a function of $\omega\Delta t$ in the range $[0, \pi]$. We note that $\omega\Delta t = 2\pi/N_{\mathrm{ppp}}$, where N_{ppp} is the number of points per period and is related to the number of points per wavelength as, $N_{\mathrm{ppw}} = \sqrt{\epsilon_\infty}\eta N_{\mathrm{ppp}}$. Thus, for $\eta \leqslant 1$, the number of points per wavelength is always less than or equal to the number of points per period. Note that the number of points per wavelength in the range $[\pi/4, \pi]$ is 8–2 points per period. We are more interested in the range $[0, \pi/4]$ which involves more than 8 points per period. To generate the plots below, we have used the representative Debye material parameter values given in (6.11).

In the plots of Fig. 5 we depict graphs of the phase error $\boldsymbol{\Phi}$ defined in (7.6) versus $\omega\Delta t$ for the $(2, 2M)$-order finite difference methods applied to the Debye model, as given in equations (6.1), for (spatial) orders $2M = 2, 4, 6, 8$ and the limiting ($M = \infty$) case. The temporal refinement factor, $h_\tau = \Delta t/\tau$, is fixed at 0.1. The left plot uses values of η set to the maximum stable value for the order, as given in (6.9), while the right plot fixes η at the maximum stable value for the limiting ($M = \infty$) case as given in (6.10) (i.e., the maximum stable value for all orders).

In both plots it appears as though the infinite-order method has the least dispersion error over a vast majority of the domain. However, looking at the intermediate orders, it is clear that at some value of $\omega\Delta t$ each higher-order method begins to have more dispersion than the next lower-order method for increasing values of $\omega\Delta t$. Generally speaking, the higher-order methods reward large N_{ppp} more than lower-order methods do but penalize low N_{ppp}. The right plot demonstrates that fixing the value of η to be constant across orders of methods tends to exaggerate this behaviour.

Figures 6 and 7 depict similar plots as in Fig. 5, except with $h_\tau = 0.01$ and 0.001, respectively. Comparing the left plots there does not appear to be much improvement in any of the higher-order methods with respect to dispersion error. Only the second-order method seems to benefit. In fact, the plots suggest that the second-order method is vastly superior to the higher-order methods. Contrast this with the stability plots in Fig. 2 that showed orders of magnitude decreases in error for all orders with corresponding decreases in discretization parameters. However, note that decreasing h_τ changes Δt,

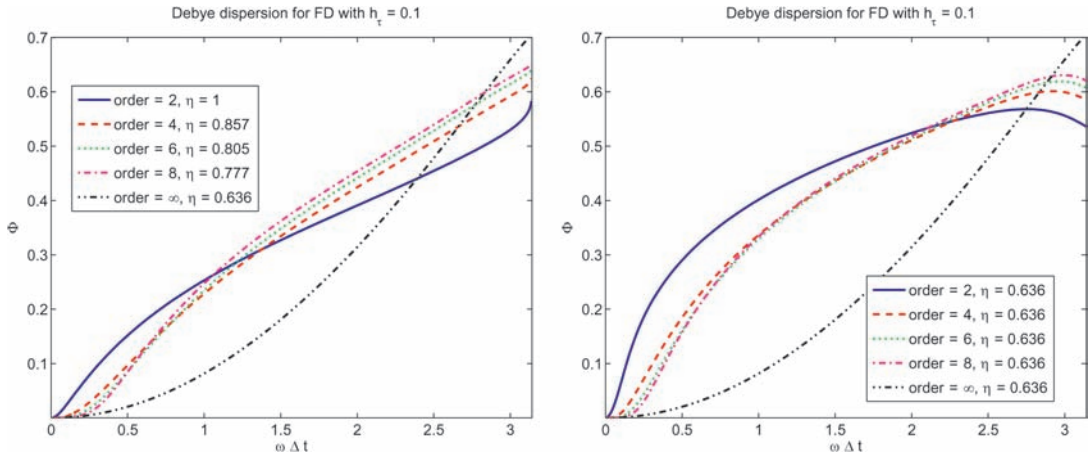

FIG. 5. (Left) Phase error ϕ versus $\omega \Delta t$ using $h_\tau = 0.1$ for the $(2, 2M)$ finite difference schemes for the Debye model, given in (6.1), of orders 2, 4, 6, 8 and the limiting ($M = \infty$) case with η set to the maximum stable value for the order, as given in (6.9). (Right) The parameter η is fixed at the maximum stable value for the limiting ($M = \infty$) case, as given in (6.10).

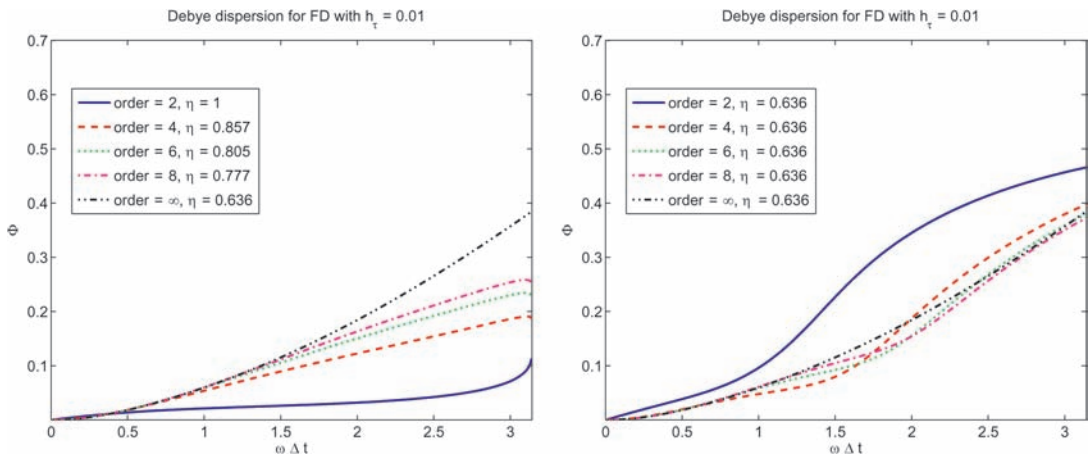

FIG. 6. Left and right plots are similar to corresponding plots in Fig. 5 except here $h_\tau = 0.01$.

thus to compare $\boldsymbol{\Phi}$ at consistent values of $\omega \Delta t$ we should be looking at different intervals in these plots.

It is more straightforward to compare various h_τ values on a plot of $\boldsymbol{\Phi}$ versus only ω as shown in Figs 8 and 9. There we can clearly see orders of magnitude decreases in $\boldsymbol{\Phi}$ as h_τ is decreased (plots using $h_\tau = 0.001$ continue this trend, see Bokil & Gibson, 2010). In fact, now it is apparent that for the frequencies of interest (i.e., those near $\omega\tau = 1$), the higher-order methods exhibit a gradual improvement over the second-order method.

Comparing left plots of Figs 5–7 with the right plots the effect of using a small Δt is that the error associated with choosing an η smaller than the maximum stable value gets magnified. In fact, it

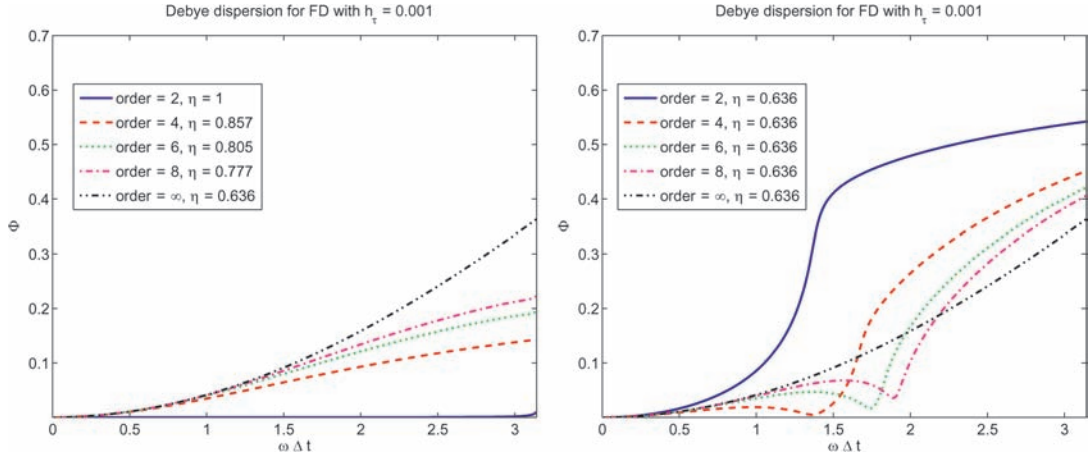

FIG. 7. Left and right plots are similar to corresponding plots in Fig. 5 except here $h_\tau = 0.001$.

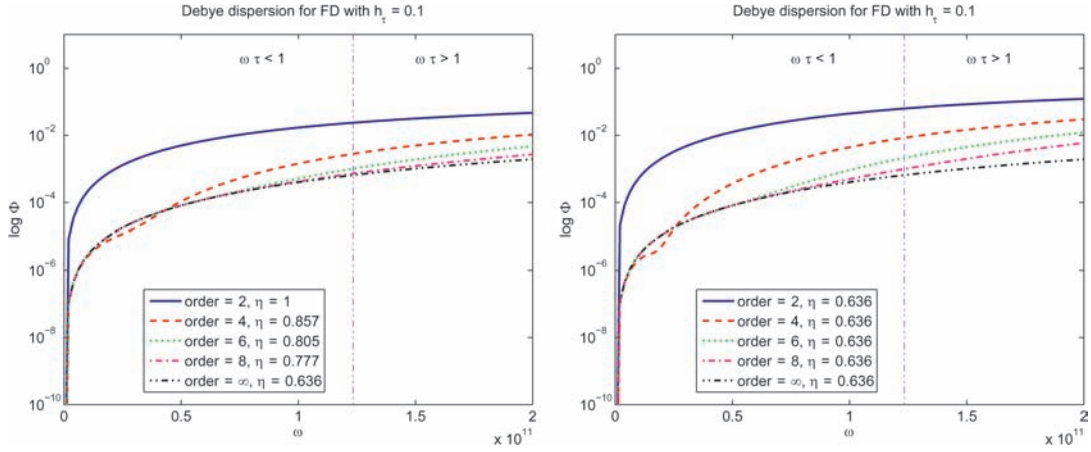

FIG. 8. Plot on left is a log plot of the phase error ϕ versus ω using $h_\tau = 0.1$ for the $(2, 2M)$ finite difference schemes for the Debye model, given in (6.1), of orders $2M = 2, 4, 6, 8$, and the limiting ($M = \infty$) case with η set to the maximum stable value for the order given in (6.9) and (6.10). Vertical line distinguishes region of $\omega\tau < 1$ from $\omega\tau > 1$. Plot on right is with η fixed at the maximum stable value for the limiting ($M = \infty$) case, as given in (6.10).

appears as though the error for the second-order method using $\eta = 0.636$ gets larger with a smaller Δt! However, again, the horizontal axis is changing from one plot to another, so the correct interpretation is that using a small Δt penalizes small N_{ppw} more so than using a larger Δt would. This is a significant point for cases that exhibit time stiffness (e.g., very different zero and infinite frequency permittivities or multi-pole models) (see Petropoulos, 1995). In simulating these systems one desires a small η, possibly such that $\Delta t = \mathcal{O}(\Delta z^2)$. The (2, 2)-order scheme has prohibitive dispersion error in the high-frequency regime for this small a value for η (the relative increase in error versus higher spatial order schemes gets worse for smaller η as shown by comparing left and right plots of Fig. 8).

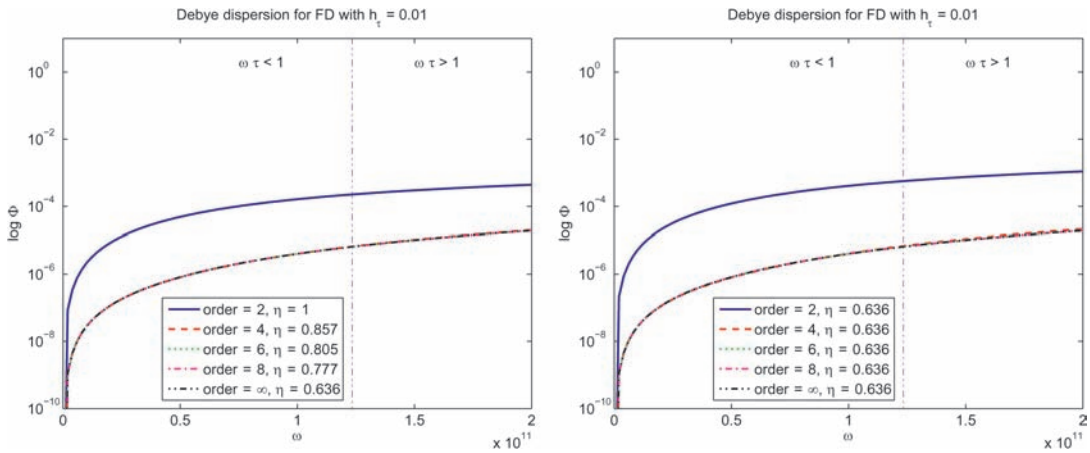

FIG. 9. Left and right plots are similar to corresponding plots of Fig. 8 except here using $h_\tau = 0.01$.

Lastly, we observe that decreasing the discretization parameter Δt results in a converging of the methods of various orders, with the notable exception of the second-order method. While Figs 6 and 7 seemed to suggest that the second-order method was vastly superior for fine discretizations, Fig. 9 contradicts that assumption utterly.

7.2 *Lorentz media*

The dispersion relation for the continuous Lorentz model, given in (2.4) (or equivalently (2.5)), is given by

$$k^{\mathrm{L}}_{\mathrm{EX}}(\omega) = \frac{\omega}{c}\sqrt{\epsilon^{\mathrm{L}}_{\mathrm{r}}(\omega)}, \quad \epsilon^{\mathrm{L}}_{\mathrm{r}}(\omega) := \frac{\omega^2\epsilon_\infty - \epsilon_{\mathrm{s}}\omega_0^2 + \mathrm{i}\,\nu\omega\epsilon_\infty}{\omega^2 - \omega_0^2 + \mathrm{i}\nu\omega}, \tag{7.7}$$

where $\epsilon^{\mathrm{L}}_{\mathrm{r}}$ is the relative complex permittivity for Lorentz media.

7.2.1 $(2, 2M)$ *KF schemes*. We consider the $(2, 2M)$ KF schemes for Lorentz media presented in equations (6.12). The numerical dispersion relation for this scheme can be computed as

$$K^{\mathrm{L}}_{\mathrm{KF},M}(\omega) = \frac{\omega_\Delta}{c}\sqrt{\epsilon^{\mathrm{L}}_{\mathrm{r,KF}}}, \quad \epsilon^{\mathrm{L}}_{\mathrm{r,KF}} := \frac{\omega_\Delta^2\epsilon_{\infty,\Delta} - \epsilon_{\mathrm{s},\Delta}\tilde{\omega}_{0,\Delta}^2 + \mathrm{i}\nu_\Delta\omega_\Delta\epsilon_{\infty,\Delta}}{\omega_\Delta^2 - \tilde{\omega}_{0,\Delta}^2 + \mathrm{i}\nu_\Delta\omega_\Delta}, \tag{7.8}$$

where the quantity $K^{\mathrm{L}}_{\mathrm{KF},M}(\omega)$ is as given in (7.2) with $k_{\Delta,M} = k^{\mathrm{L}}_{\mathrm{KF},M}$. In the above, $k^{\mathrm{L}}_{\mathrm{KF},M}$ is the numerical wave number, and $\epsilon^{\mathrm{L}}_{\mathrm{r,KF}}$ is the discrete relative complex permittivity for the $(2, 2M)$ KF schemes. The discrete representations of the continuous model parameters ϵ_{s}, ϵ_∞ and ω are as defined in (7.4) and (7.5), the discrete resonance frequency $\tilde{\omega}_{0,\Delta}$ is defined as

$$\tilde{\omega}_{0,\Delta} := \omega_0 \cos(\omega\Delta t/2), \tag{7.9}$$

and the discrete representation of the damping coefficient ν is

$$\nu_\Delta := \nu \cos(\omega\Delta t/2). \tag{7.10}$$

7.2.2 $(2, 2M)$ *JHT schemes.* We consider the $(2, 2M)$ JHT schemes for Lorentz media presented in equations (6.21). The numerical dispersion relation for these schemes can be computed as

$$K^{\mathrm{L}}_{\mathrm{JHT},M}(\omega) = \frac{\omega_{\Delta}}{c}\sqrt{\epsilon^{\mathrm{L}}_{\mathrm{r,JHT}}}, \quad \epsilon^{\mathrm{L}}_{\mathrm{r,JHT}} := \frac{\omega^2_{\Delta}\epsilon_{\infty,\Delta} - \epsilon_{\mathrm{s},\Delta}\omega^2_{0,\Delta} + \mathrm{i}\nu_{\Delta}\omega_{\Delta}\epsilon_{\infty,\Delta}}{\omega^2_{\Delta} - \omega^2_{0,\Delta} + \mathrm{i}\nu_{\Delta}\omega_{\Delta}}, \tag{7.11}$$

where the quantity $K^{\mathrm{L}}_{\mathrm{JHT},M}(\omega)$ is as given in (7.2) with $k_{\Delta,M} = k^{\mathrm{L}}_{\mathrm{JHT},M}$. In the above, $k^{\mathrm{L}}_{\mathrm{JHT},M}$ is the numerical wave number, and $\epsilon^{\mathrm{L}}_{\mathrm{r,JHT}}$ is the discrete relative complex permittivity for the $(2, 2M)$ JHT schemes. The discrete representations of the continuous model parameters ϵ_{s}, ϵ_{∞}, ω and ν are as defined in (7.4), (7.5) and (7.10) and the discrete resonance frequency $\omega_{0,\Delta}$ (different from $\tilde{\omega}_{0,\Delta}$ for the $(2, 2M)$ KF schemes) is defined as

$$\omega_{0,\Delta} := \omega_0\sqrt{\cos(\omega\Delta t)}. \tag{7.12}$$

7.2.3 *Phase error of KF and JHT schemes.* In this section, we analyse plots of the phase error $\boldsymbol{\Phi}$ for the $(2, 2M)$-order KF and the JHT finite difference schemes applied to Lorentz media. The phase error is as defined in (7.6) where now k_{EX} is given by (7.7) and $k_{\Delta,M}$ is either $k^{\mathrm{L}}_{\mathrm{KF},M}$ or $k^{\mathrm{L}}_{\mathrm{JHT},M}$. The phase error is plotted against values of $\omega\Delta t$ in the range $[0, \pi]$. To generate the plots below we have used the representative Lorentz model material parameters given in (6.20).

In the plots of Fig. 10 we depict graphs of the phase error $\boldsymbol{\Phi}$ defined in (7.6), versus $\omega\Delta t$, for the $(2, 2M)$-order KF methods applied to the Lorentz model, given in equations (6.12), for (spatial) orders $2M = 2, 4, 6, 8$ and the limiting ($M = \infty$) case. The temporal refinement factor, $h_0 = \Delta t/\omega_0$, is fixed at 0.1. The left plot uses values of η set to the maximum stable value for the order, while the right plot fixes η at the maximum stable value for the limiting ($M = \infty$) case (i.e., the maximum stable value for all orders). These bounds for η are given in (6.19).

The qualitative behaviour of the curves is much different here than for the Debye model depicted in Fig. 5, however, the basic result is the same. That is, the infinite-order method has the least dispersion

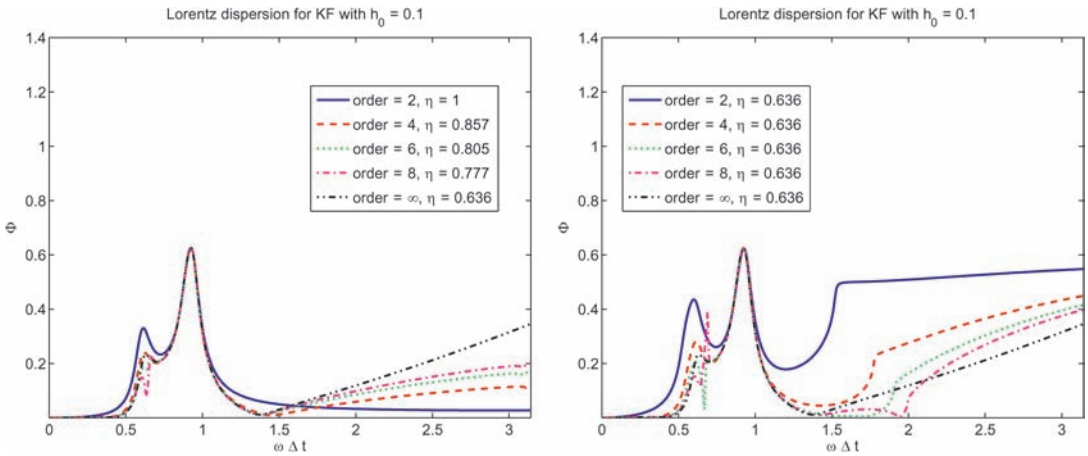

FIG. 10. (Left) Phase error ϕ versus $\omega\Delta t$ using $h_0 = 0.1$ for the $(2, 2M)$ KF scheme for the Lorentz model, given in equations (6.12), of orders $2M = 2, 4, 6, 8$ and the limiting ($M = \infty$) case with η set to the maximum stable value for the order. Plot on right is with η fixed at the maximum stable value for the limiting ($M = \infty$) case, where the bounds for η are given in (6.19).

for the vast majority of refinement values of interest, and in general, at some value of $\omega \Delta t$ each higher-order method begins to have more dispersion than the next lower-order method for increasing values of $\omega \Delta t$. For the right plot of Fig. 10 the behaviour of the curves for high $\omega \Delta t$ is instead dominated by the restriction of η. In particular, the second-order method has very large dispersion for $\omega \Delta t > 1.5$. This result does not change as the temporal refinement, h_0 is decreased, as was the case for the Debye model (see the right plot in Fig. 11, where $h_0 = 0.01$ and compare to Fig. 7 for the Debye model).

The left plot in Fig. 11 also was generated with $h_0 = 0.01$ and demonstrates that the dispersion for large $\omega \Delta t$ did not improve for the higher-order methods. In fact, decreasing h_0 even further has no effect: plots with $h_0 = 0.001$ are interesting in that there is almost no change from the previous case (see Bokil & Gibson, 2010). In particular, the left plot of Fig. 11 suggests that the second-order method with $\eta = 1$ is far superior to all other orders of methods for the $(2, 2M)$ KF schemes applied to the Lorentz polarization model.

In the plots of Fig. 12 we depict graphs of the phase error $\boldsymbol{\Phi}$ defined in (7.6), versus $\omega \Delta t$, for the $(2, 2M)$-order JHT finite difference methods applied to the Lorentz model, given in equations (6.21), for (spatial) orders $2M = 2, 4, 6, 8$ and the limiting ($M = \infty$) case. Again, the temporal refinement factor, $h_0 = \Delta t/\omega_0$, is fixed at 0.1. The qualitative behaviour of the curves here is very similar to those of the corresponding $(2, 2M)$ KF schemes depicted in Fig. 10, with the notable exception of the dispersion for large $\omega \Delta t$. For the $(2, 2M)$ JHT schemes both the left and right plots exhibit large dispersion errors for the lower-order methods for $\omega \Delta t > 1.5$. This was noted in Petropoulos (1994) for the $(2, 2)$ JHT scheme and cited as a reason to prefer the $(2, 2)$ KF scheme. Note that this is a direct result of the stability constraint on the $(2, 2M)$ JHT schemes in that $\eta < 1$ even for the second-order method. Interestingly, there is no value of $\omega \Delta t$ at which each higher-order method begins to have more dispersion than the next lower-order method for increasing values of $\omega \Delta t$ as was the case for the Debye model and the KF scheme for Lorentz.

The dispersion curves for the $(2, 2M)$ JHT schemes using $h_0 = 0.01$ with $\eta = 0.45$ fixed have the same qualitative structure as those corresponding to the KF scheme depicted in the right plot of Fig. 11. However, due to the stability constraints for the $(2, 2M)$ JHT schemes, the curves using the largest stable

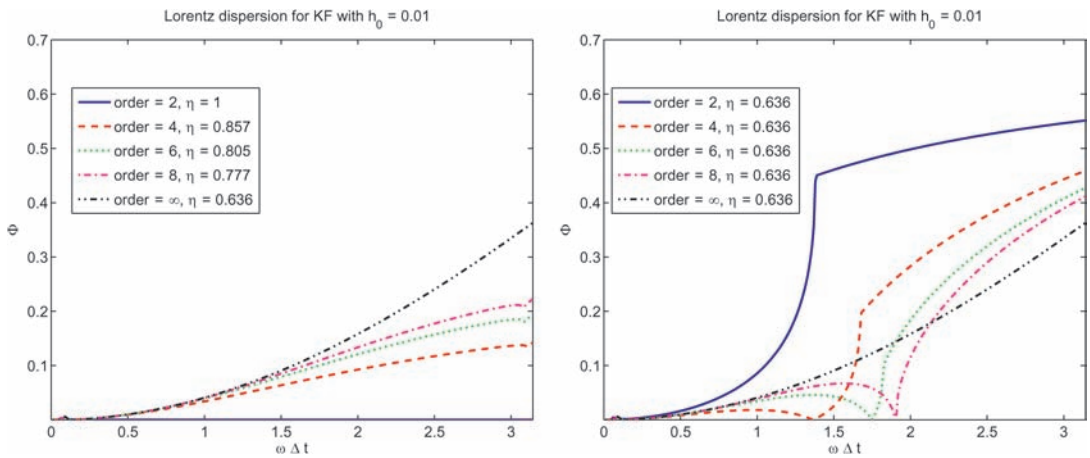

FIG. 11. Left and right plots are similar to corresponding plots in Fig. 10 except here $h_0 = 0.01$. Note the change in axes from that of Fig. 10.

values of η at each order also have large phase errors for large $\omega \Delta t$ making the left and right plots nearly indistinguishable in these cases (see Bokil & Gibson, 2010).

It would appear from comparing all the dispersion curves for KF and JHT schemes that the second-order KF scheme is preferable for all temporal refinements $h_0 \leqslant 0.01$. However, again we note that decreasing h_0 changes Δt, thus to compare consistent quantities we should compare various h_0 values on a plot of $\boldsymbol{\Phi}$ versus only ω as shown in Figs 13 and 14. There we can clearly see orders of magnitude

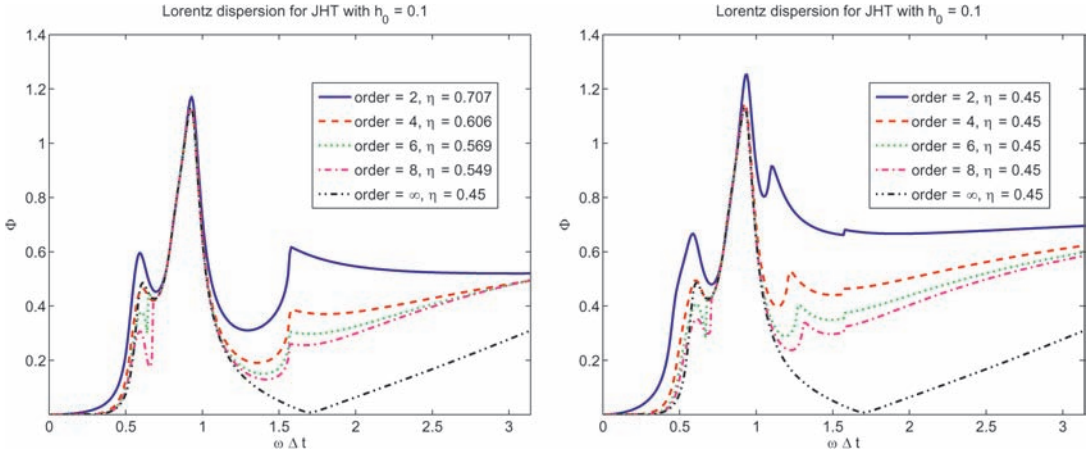

FIG. 12. (Left) Phase error ϕ versus $\omega \Delta t$ using $h_0 = 0.1$ for the $(2, 2M)$ JHT scheme for the Lorentz model, given in equations (6.21), of orders $2M = 2, 4, 6, 8$ and the limiting ($M = \infty$) case. The parameter η is set to the maximum stable value for the order as given in (6.29). (Right) The parameter η fixed at the maximum stable value for the limiting ($M = \infty$) case as given in (6.29).

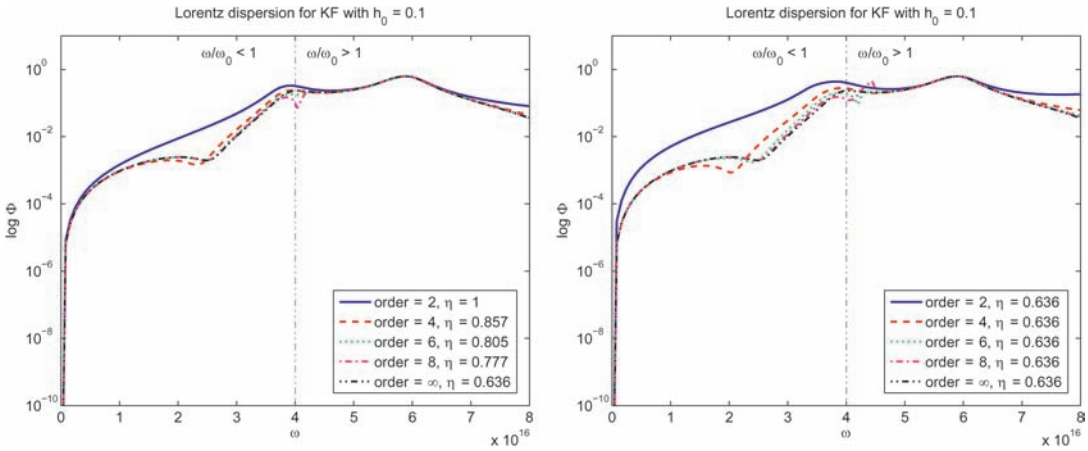

FIG. 13. Plot on left is a log plot of the phase error ϕ versus ω using $h_0 = 0.1$ for the $(2, 2M)$ KF scheme for the Lorentz model, given in equations (6.12a)–(6.12d), of orders $2M = 2, 4, 6, 8$ and the limiting ($M = \infty$) case with η set to the maximum stable value for the order as given in (6.19). Vertical line distinguishes region of $\omega/\omega_0 < 1$ from $\omega/\omega_0 > 1$. Plot on right is with η fixed at the maximum stable value for the limiting ($M = \infty$) case as given in (6.19).

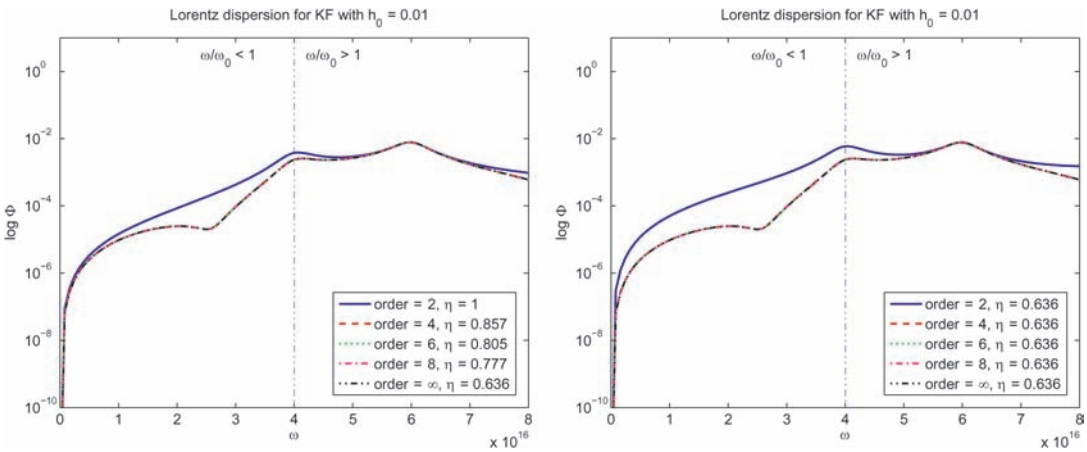

FIG. 14. Left and right plot are similar to corresponding plots of Fig. 13 except here $h_0 = 0.01$.

decreases in $\boldsymbol{\Phi}$ for the frequencies of interest (i.e., those near $\omega/\omega_0 = 1$) as h_ν is decreased (the trend continues for $h_0 = 0.001$ as shown in Bokil & Gibson, 2010). Note that there is significantly less difference between the high frequency dispersion in the JHT scheme versus the KF scheme even for the second-order method, than the $\omega \Delta t$ plots suggested, as the corresponding plots are nearly indistinguishable (see Bokil & Gibson, 2010). Lastly, now it is apparent that each of the higher-order methods exhibits a significant improvement over the second-order method (for some frequencies, at least an order of magnitude), however, there is little accuracy gained by orders > 4 except for the very highest frequencies and for large values of h_0.

8. Conclusions

We have studied staggered finite difference schemes of arbitrary (even-) order in space and second-order in time for dispersive materials (Debye and Lorentz) and compared them from the point of view of stability and dispersion. This study was inspired by the work in Petropoulos (1994) for second-order methods.

For each scheme we have given a necessary and sufficient stability condition which is explicitly dependent on the material parameters and the order of the method. Additionally, we have found a bound for stability for all orders by computing the limiting (infinite-order) case. Further, we have derived a concise representation of the numerical dispersion relation for each scheme of arbitrary order, which allows an efficient method for predicting the numerical characteristics of a simulation of electromagnetic wave propagation in a dispersive material.

From the stability analysis in the paper, we can conclude that the numerical dissipation in the schemes presented here for Debye and Lorentz media are strongly dependent on the temporal resolution (the quantity $h_\tau = \Delta t/\tau$ when τ is the smallest time scale for Debye media, and for Lorentz media, either the quantity $h_0 = \omega_0 \Delta t/2\pi$ or $h_\nu = \nu \Delta t$, whichever is the more restrictive quantity depending on the relative values of $2\pi/\omega_0$ and $1/\nu$). We see that h_τ for Debye, and h_0 or h_ν for Lorentz have to be sufficiently small in order to accurately model the propagation of pulses at large distances inside the dispersive dielectric medium. For higher orders the stability restriction has the effect of allowing larger wave numbers to exhibit the same dissipation error as would a smaller wave number at a lower order.

From the dispersion analysis, we see that the discrete representations of the continuous model parameters are the same regardless of spatial order of the method, only the representation of the wave number changes. Numerical experiments show that the dispersion error for fourth-order methods is slightly less than that of second-order methods, but no significant gain, with respect to dispersion error, is achieved by increasing to order higher than 4.

Other higher-order methods for dispersive materials may also be analysed using the approaches described in the current work, including those for the Drude polarization model, the stable-JHT scheme described in Pereda *et al*. (2001), those corresponding to collisionless cold plasma Young (1996) and others which are mentioned in Bidégaray-Fesquet (2008). Additionally, any number of multiple poles may be considered in a straightforward manner, see, for example, the fourth- and sixth-order methods for multi-pole Debye and Lorentz in Prokopidis & Tsiboukis (2006). The specific stability results from Bidégaray-Fesquet (2008) for two and three dimensions may be extended as well in a similar fashion to the analysis presented here by using a representation of the numerical schemes in a manner as described in Cohen (2001) for the wave equation.

Acknowledgements

The first author is supported by a grant from the National Science Foundation (NSF) Computational Mathematics program, proposal number DMS-0811223 and by the grant CMG EAR-0724865 from the NSF's Collaborations in Mathematical Geosciences program. The authors would like to thank an anonymous referee for very helpful comments and suggestions.

References

ANNE, L., JOLY, P. & TRAN, Q. H. (2000) Construction and analysis of higher order finite difference schemes for the 1D wave equation. *Comput. Geosci*., **4**, 207–249.

BANKS, H. T., BOKIL, V. A. & GIBSON, N. L. (2009) Analysis of stability and dispersion in a finite element method for Debye and Lorentz dispersive media. *Numer. Methods Partial Differ. Equ*., **25**, 885–917.

BANKS, H. T., BUKSAS, M. W. & LIN, T. (2000) *Electromagnetic Material Interrogation Using Conductive Interfaces and Acoustic Wavefronts*. Frontiers in Applied Mathematics, vol. FR21. Philadelphia, PA: SIAM.

BIDÉGARAY-FESQUET, B. (2008) Stability of FD-TD schemes for Maxwell–Debye and Maxwell–Lorentz equations. *SIAM J. Numer. Anal*., **46**, 2551–2566.

BOKIL, V. A. & GIBSON, N. G. (2010) High-order staggered finite difference methods for Maxwell's equations in dispersive media. *Technical Report ORST-MATH-10-01*. Oregon State University. Available at http://hdl.handle.net/1957/13786.

BRILLOUIN, L. (1960) *Wave Propagation and Group Velocity*. New York: Academic Press.

COHEN, G. C. (2001) *Higher-Order Numerical Methods for Transient Wave Equations*. Berlin: Springer.

CUMMER, S. A. (1997) An analysis of new and existing FDTD methods for isotropic cold plasma and a method for improving their accuracy. *IEEE Trans. Antenn. Propag*., **45**, 392–400.

FEAR, E. C., MEANEY, P. M. & STUCHLY, M. A. (2003) Microwaves for breast cancer detection. *IEEE Potentials*, **22**, 12–18.

FORNBERG, B. (1975) On a Fourier method for the integration of hyperbolic equations. *SIAM J. Numer. Anal*., **12**, 509–528.

FORNBERG, B. (1990) High-order finite differences and the pseudospectral method on staggered grids. *SIAM J. Numer. Anal*., **27**, 904–918.

FORNBERG, B. & GHRIST, M. (1999) Spatial finite difference approximations for wave-type equations. *SIAM J. Numer. Anal*., **37**, 105–130.

GHRIST, M. (2000) Finite difference methods for wave equations. *Ph.D. Thesis*, University of Colorado, Boulder, CO.

JOSEPH, R. M., HAGNESS, S. C. & TAFLOVE, A. (1991) Direct time integration of Maxwell's equations in linear dispersive media with absorption for scattering and propagation of femtosecond electromagnetic pulses. *Optics Lett.*, **16**, 1412–1414.

KASHIWA, T. & FUKAI, I. (1990) A treatment by the FD-TD method of the dispersive characteristics associated with electronic polarization. *Microwave Opt. Technol. Lett.*, **3**, 203–205.

KASHIWA, T., YOSHIDA, N. & FUKAI, I. (1990) A treatment by the finite-difference time-domain method of the dispersive characteristics associated with orientation polarization. *IEEE Trans. IEICE*, **73**, 1326–1328.

PEREDA, A., VIELVA, L. A., VEGAS, A. & PRIETO, A. (2001) Analyzing the stability of the FDTD technique by combining the von Neumann method with the Routh–Hurwitz criterion. *IEEE Trans. Microwave Theory Techniques*, **49**, 377–381.

PETROPOULOS, P. G. (1994) Stability and phase error analysis of FD-TD in dispersive dielectrics. *IEEE Trans. Antenn. Propag.*, **42**, 62–69.

PETROPOULOS, P. G. (1995) The wave hierarchy for propagation in relaxing dielectrics. *Wave Motion*, **21**, 253–262.

PROKOPIDIS, K. P., KOSMIDOU, E. P. & TSIBOUKIS, T. D. (2004) An FDTD algorithm for wave propagation in dispersive media using higher-order schemes. *J. Electromagnet. Waves Appl.*, **18**, 1171–1194.

PROKOPIDIS, K. P. & TSIBOUKIS, T. D. (2004) FDTD algorithm for microstrip antennas with lossy substrates using higher order schemes. *Electromagnetics*, **24**, 301–315.

PROKOPIDIS, K. P. & TSIBOUKIS, T. D. (2006) Higher-order spatial FDTD schemes for EM propagation in dispersive media. *Electromagnetic Fields in Mechatronics, Electrical and Electronic Engineering: Proceedings of ISEF'05* (A. Krawczyk, S. Wiak & X. M. López-Fernández eds). Studies in Applied Electromagnetics and Mechanics, vol. 27. Amsterdam, The Netherlands: IOS Press, pp. 240–246.

SIUSHANSIAN, R. & LOVETRI, J. (1995) A comparison of numerical techniques for modeling electromagnetic dispersive media. *IEEE Microwave Guided Wave Lett.*, **5**, 426–428.

STRIKWERDA, J. C. (2004) *Finite Difference Schemes and Partial Differential Equations*. Philadelphia, PA: SIAM.

TAFLOVE, A. & HAGNESS, S. C. (2005) *Computational Electrodynamics: The Finite-Difference Time-Domain Method*, 3rd edn. Norwood, MA: Artech House.

TREFETHEN, L. N. (1982) Group velocity in finite difference schemes. *SIAM Rev.*, **24**, 113–136.

YOUNG, J. (1996) A higher order FDTD method for EM propagation in a collisionless cold plasma. *IEEE Trans. Antenn. Propag.*, **44**, 1283–1289.

YOUNG, J., GAITONDE, D. & SHANG, J. (1997) Toward the construction of a fourth-order difference scheme for transient EM wave simulation: staggered grid approach. *IEEE Trans. Antenn. Propag.*, **45**, 1573–1580.

YOUNG, J. L., KITTICHARTPHAYAK, A., KWOK, Y. M. & SULLIVAN, D. (1995) On the dispersion errors related to $(FD)^2TD$ type schemes. *IEEE Trans. Microwave Theory Techniques*, **43**, 1902–1910.

YOUNG, J. L. & NELSON, R. O. (2001) A summary and systematic analysis of FDTD algorithms for linearly dispersive media. *IEEE Antenn. Propag. Mag.*, **43**, 61–77.